HEAT TRANSFER TO NANOFLUIDS FLOW IN VARIABLE CIRCULAR AND ANNULAR PASSAGE CONFIGURATION

ARRUL A/L JAGINDAR

FACULTY OF ENGINEERING

UNIVERSITY OF MALAYA

KUALA LUMPUR

2021

Universiti Malaya

UNIVERSITY OF MALAYA

ORIGINAL LITERARY WORK DECLARATION

Name of Candidate: Arrul a/l Jagindar

Matric No: KQK180038

Name of Degree: Master of Mechanical Engineering

Title of Project Paper/Research Report/Dissertation/Thesis ("this Work"):

Heat transfer to Nanofluids flow in variable Circular and Annular Passage Configuration

Field of Study: Heat Exchanger

I do solemnly and sincerely declare that:

(1) I am the sole author/writer of this Work;
(2) This Work is original;
(3) Any use of any work in which copyright exists was done by way of fair dealing and for permitted purposes and any excerpt or extract from, or reference to or reproduction of any copyright work has been disclosed expressly and sufficiently and the title of the Work and its authorship have been acknowledged in this Work;
(4) I do not have any actual knowledge nor do I ought reasonably to know that the making of this work constitutes an infringement of any copyright work;
(5) I hereby assign all and every rights in the copyright to this Work to the University of Malaya ("UM"), who henceforth shall be owner of the copyright in this Work and that any reproduction or use in any form or by any means whatsoever is prohibited without the written consent of UM having been first had and obtained;
(6) I am fully aware that if in the course of making this Work I have infringed any copyright whether intentionally or otherwise, I may be subject to legal action or any other action as may be determined by UM.

Candidate's Signature: Date:21/7/2021

Subscribed and solemnly declared before,

Witness's Signature Date:

Name:

Designation:

University of Malaya

ABSTRACT

The invention of the heat exchanger is widely regarded as one of the most significant inventions of all time. Heat exchangers are critical pieces of equipment used in a variety of industrial settings, including power plants, the HVAC sector, and the chemical industry. In heat exchangers, numerous fluids are employed as working fluids. Water, oil, and ethylene glycol are three of the most often utilized working fluids.A minor alteration in the operating principle of a heat exchanger can produce a significantly larger result at a lower cost. This concept has always piqued the interest of scholars. As a result, researchers have done several studies to improve the heat exchanger, whether from a material or heat transfer standpoint.

In terms of heat transfer, they discovered that traditional working fluids have limited thermal conductivity and characteristics. There have been attempts to make a combination of solid particles suspended in water. This invention suffered a setback when the pressure drop was impaired, sedimentation developed, or even erosion happened, resulting in higher maintenance costs.

Gago and TioSio nanofluids were synthesized in this study investigated their performance in heat exchanger applications. Thermophysical characteristics, thermal conductivity, specific heat capacity were measured.The heat transfer coefficients were investigated at fully developed turbulent flow regime in an annular tube heat exchanger .

The experimental data of all the synthesized nanofluids showed a considerable increase in thermal conductivity and heat transfer coefficient when compared with the results obtained from the base fluid. Based on the experimental results, several improved empirical correlations for calculating the Nusselt number and friction factor were proposed in this study.

Keywords: Heat exchanger, Nanofluids, Heat transfer Coefficient, Nusselt number, Pressure Drop, Thermo-physical.

Universiti Malaya

ABSTRAK

Penemuan penukar haba secara meluas dianggap sebagai salah satu penemuan paling penting sepanjang masa. Penukar haba adalah peralatan penting yang digunakan dalam pelbagai tetapan industri, termasuk loji janakuasa, sektor HVAC, dan industri kimia. Dalam penukar haba, banyak cecair digunakan sebagai cecair berfungsi. Air, minyak, dan etilena glikol adalah tiga cecair kerja yang paling sering digunakan. Perubahan kecil dalam prinsip operasi penukar haba dapat menghasilkan hasil yang jauh lebih besar dengan biaya yang lebih rendah. Konsep ini sentiasa menarik minat para sarjana. Hasilnya, penyelidik telah melakukan beberapa kajian dan penyelidikan untuk meningkatkan penukar haba, baik dari sudut bahan atau pemindahan haba.

Dari segi pemindahan haba, mereka mendapati bahawa cecair kerja tradisional mempunyai kekonduksian dan ciri haba yang terhad. Terdapat percubaan untuk membuat gabungan zarah pepejal yang terampai di dalam air. Penemuan ini mengalami kemunduran ketika penurunan tekanan terganggu, pemendapan berkembang, atau bahkan hakisan berlaku, mengakibatkan kos penyelenggaraan lebih tinggi.

Nanofluid Gago dan TioSio akan dihasilkan dalam kajian ini. Ciri termofizik, kekonduksian terma, ketumpatan, kelikatan, kapasiti haba tertentu, dan pekali pemindahan haba akan diselidiki. Aliran nanofluid akan bergelora dan berkembang sepenuhnya dalam tiub bulat dan Annular.

Data eksperimen untuk semua nanofluid yang dihasilkan menunjukkan peningkatan yang besar dalam kekonduksian terma dan pekali pemindahan haba jika dibandingkan dengan hasil untuk cairan basa IV yang sesuai. Berdasarkan hasil eksperimen, beberapa korelasi empirikal yang lebih baik untuk mengira bilangan Nusselt dan faktor geseran dicadangkan dalam kajian ini.

Kata kunci: Penukar haba, Nanofluid, Pekali pemindahan haba, nombor Nusselt, Penurunan Tekanan, Termo-fizikal.

Universiti Malaya

ACKNOWLEDGEMENTS

First and foremost, I would want to express my heartfelt thanks to my supervisor, Prof. Dr. Kazi Md Salim Newaz, for his guidance and support in completing my thesis.

Secondly, I'd like to thank Dr. Waqar Ahmad for guiding me through the experimental investigation, simulation, and thesis writing processes. When things were tough and uncertain, he gave me advice on how to find solutions.

My thanks also extends to all of the lecturers who shared their experience and skills with me in order to provide me with significant exposure in this field.

Last But Not Least, I'd like to express my gratitude to my family and friends for their unwavering support. Without them, we would not have made it to the end of the tunnel and seen the light of day. Thank you.

Universiti Malaya

TABLE OF CONTENTS

Universiti Malaya

Universiti Malaya

Universiti Malaya

Universiti Malaya

Universiti Malaya

LIST OF FIGURE

Universiti Malaya

Universiti Malaya

Universiti Malaya

Universiti Malaya

LIST OF TABLES

Universiti Malaya

Universiti Malaya

LIST OF SYMBOLS AND ABBREVIATIONS

C*f*	:	Friction coefficient
C*p*	:	Specific Heat, KJ/kg·K
DW	:	Distilled Water
F	:	Friction factor
H	:	Convection heat transfer coefficient, W/m2 ·K
K	:	Thermal Conductivity, W/m·K
Nu	:	Nusselt number
Re	:	Reynolds number
T	:	Temperature, K
P	:	Pressure, Pa
T*b*	:	Fluid bulk temperature, K
T*w*	:	Tube wall temperature, K
U	:	Velocity component in x direction, m/s
V	:	Velocity component in y direction, m/s

Universiti Malaya

CHAPTER 1: INTRODUCTION

1.1 Background

Heat Transfer enhancement is an interesting topic that has been widely researched throughout the globe. The possibility of using nanofluid and nanoparticles to enhance the Heat transfer properties has driven the interest of many researchers. Application of heat transfer in engineering depend upon a few factors such as size and weight. The increase in efficiency can reduce the initial setup cost. (Ha, Jeon, Choi, & Kim; Kakavandi & Akbari; Ueki, Fujita, Kawai, & Shibahara)

1.2 Working Fluid

The common working fluid in a heat exchanger can be identified as oil, water and ethylene glycerol. These fluids exhibit advantages in terms of ease of handling, recycling and disposing. Besides that, it has a low market price. Despite the advantages listed, these fluids are exhibits low thermal properties. Moreover, characteristic such as fouling and less surface energy makes the entire heat transfer's efficiency low resulting in the design of heat exchanger to be larger so that desired energy can be harnessed for the operations in the time duration (Zubir et al.).

Therefore, efforts have been taken to identify fluid that can increase the heat transfer performance (Åkerstedt, Högberg, & Lundström, 2013).Notable technique used to improvise the fluid properties is by addition of particles in order to form double-phase fluid slurries. Example of substance mixed with the base fluid are Hitherto, micron particles such as metal, non-metal and polymeric .

Universiti Malaya

In this study, (GAGO) are used as working fluid to improve the efficiency of the heat exchanger. The better thermal conductivity exhibited by this solution helps the increase of heat transfer rate. (A. Amiri et al., 2015; Kazi, Duffy, & Chen, 1999; X. Wang et al., 2007).

1.3 Heat Exchanger

A heat exchanger is a device that allows heat to be transferred from one fluid to another.. Depending on the type of exchanger, the fluids can be single or two phase, separated or in direct contact. Despite the fact that many of the principles involved in their design are the same, systems that use energy sources such as nuclear fuel pins or fired heaters are not commonly referred to be heat exchangers.(Huminic & Huminic, 2012).

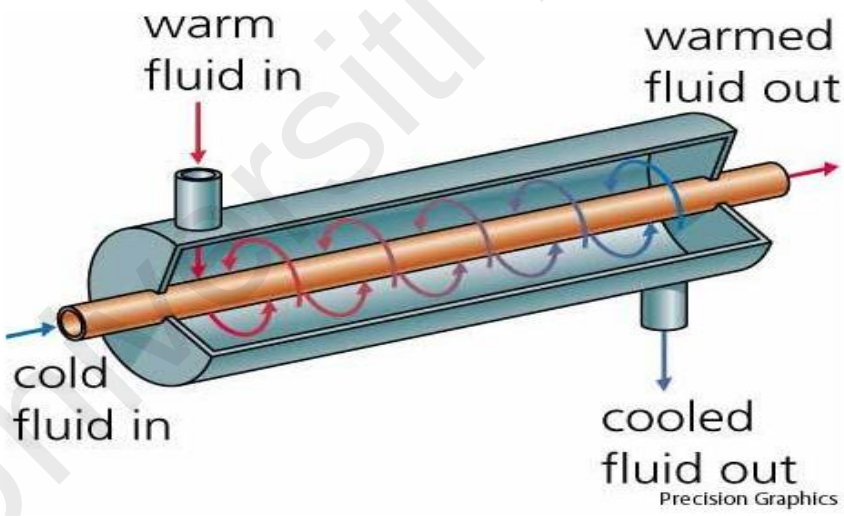

Figure 1.1: Working Principle of Heat Exchanger (Encyclopædia Britannica, Inc)

Universiti Malaya

The rising cost of energy has compelled enterprises to implement energy-saving measures in their facilities. The efforts were concentrated on

1. Enhancement in heat transfer of heat exchanger
2. Reduction of heat transfer time
3. Improvisation of efficiency and energy utilization.

The efficiency of the heat exchanger can be increased by two parameters that are being investigated here. First, the geometry of the heat exchanger is investigated and how it can be improved, followed by an investigation of the working fluid in the heat exchanger, in which the thermal properties of the working fluid are tested as a manipulated variable.These methods are known as the passive method to improve the heat transfer performance(Nakhchi & Esfahani, 2019).

1.4 What is Nanofluid

Nanofluid is described as a fluid containing nanometer-sized particles known as nanoparticles. Colloidal suspension occurs when these particles are equally and stably suspended in a fluid. Nanofluids should be evaluated as a promising future heat transfer application. Various nanomaterials have been investigated over the last decade for heat transfer applications, with parameters such as volume fraction, size, thermal characteristics, and shape having a significant impact on heat transfer coefficient and thermal conductivity when suspended in a base fluid.(Bhanvase, Barai,Sonawane, Kumar, & Sonawane, 2018).

Universiti Malaya

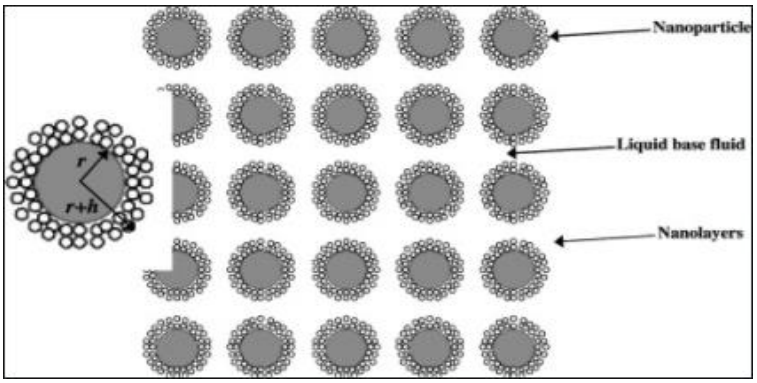

Figure 1.2: The structure of a nanofluid(heatmass transfer vol10.2009)

Fluids having solid nanometer-sized particle dispersion are referred to as "nanofluids." The single-phase modelling, which considers the mixture of nanoparticles and base fluid as a single-phase mixture with stable properties, and the two-phase modelling, in which the nanoparticle properties and behaviours are considered separately from the base fluid, were both thoroughly discussed.

The study found that the nanoparticles present in the base fluid improves the fluid's thermal conductivity. This could be used in a variety of fields within the industry.(Aly, 2014; Choi & Eastman, 1995)Tin Oxide (TiO2), Aluminium Oxide (Al2O3), Copper Oxide (CuO) and Zinc Oxide (ZnO) were examined in the past to be used in nanofluid (Khoshvaght-Aliabadi, 2014).

Later, materials that are carbon based such as CNT, GO (Taha-Tijerina, M. Sudeep,Ajayan, Narayanan, & Anantharamaniyer, 2014), and Graphene were experimentally analysed. Nanofluid is seen as an alternative working fluid because its enhanced thermal properties. (Ahmad Amiri et al.,2015)

In recent years, carbon-based nanomaterials have been tested to improve the efficiency of the working fluid. In the literature of Ding et al., graphene platelets were purportedly employed to make nanofluid. When compared to other nanofluids, the results revealed an increase in thermal

Universiti Malaya

conductivity. The properties of carbon-based materials are excellent. (Ding, Alias, Wen, & Williams, 2006)

1.4.1 Types of Nanofluid

Nanofluids are derived into 4 types according to the type of dispersed particle: (1) metal, (2) metal oxide, (3) carbon, and (4) metal hybrid. To form nanofluids, These nanoparticles are suspended in a variety of host fluids, including water, ethylene glycol, oils, and methanol.

1.4.2 Nanofluid Preparation

Nanofluid preparation can be classified into "one - step" and "two - step" approaches. The one-step process entails spreading nanoparticles directly into the base fluids while producing them. nanoparticles, and the creation of nanoparticles and nanofluids occurs concurrently. The nanofluid generated in a single step possesses small particle size, good dispersion, and high suspension.The single step method involves producing the nanofluid and nanoparticle directly from physical vapour deposition method. This process has a limitation where only it is only applicable to low vapour pressure fluids (Y. Li, Zhou, Tung, Schneider, & Xi, 2009).

Meanwhile, the two-step approach entails dispersing nanoparticles in a base fluid. Mechanical alloying, inert gas condensation, and chemical vapour deposition are all processes used to create dry nanoparticles. After producing dry nanoparticles, they are distributed in a liquid. Agglomeration is the process through which particles bind together to create aggregates.
This is a problem for this strategy since it reduces thermal conductivity. Thermal characteristics deteriorate due to channel sedimentation and obstruction. Nonetheless, there are strategies for

Universiti Malaya

reducing agglomeration and increasing dispersion. The addition of a surfactant, which enhances the particle's charge, is followed by the functionalization of the nanoparticles.In the industry, nano particles are being synthesised in massive quantities. Using the two-step process, this could be a cost-cutting technique. (Hong, Hong, & Yang, 2006).

1.5 Stability of Nanofluid

The stability of the suspension is critical in nanofluid applications. Because of the high van der Waals forces between the nanoparticles, agglomeration develops in nanofluid. The thermal and heat transfer conductivity of nanofluids is harmed by the homogeneous suspension.

A study was carried out to determine whether aggregation and clustering are factors that contribute to the improvement of thermal conductivity, thereby establishing a relationship between thermal conductivity and fluid stability. (Evans et al., 2008). Stability of nanofluid can be enhanced by methods (Ghadimi, Rahman, & Metselaar, 2011) such as:

1. Surface Chemical Treatment
2. Surfactant Addition
3. Ultrasonic Vibration

Universiti Malaya

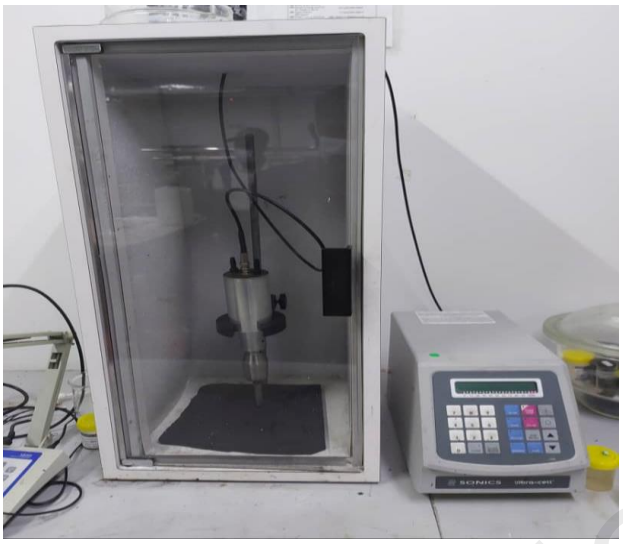

Figure 1.3: Probe Sonicator to carry out ultrasonic vibration

1.5.1 Surface Chemical Treatment

The charge and electrokinetic properties of the aqueous nanofluid have an effect on its stability. A well-homogeneous dispersed suspension can be greatly stabilised by increasing the surface charge density and the repulsive force (Wang, Zhu, &Yang et al., 2009).Because of the presence of the hydroxy functional group, acid treatment can stabilise the solution by changing the surface nature from hydrophobic to hydrophilic. (Xie, Lee, Youn, & Choi, 2003). The Isoelectric Point (IEP) theory can help to explain this. The higher the surface charge increases, the further the pH of the nanofluid from the IEP point. This is due to the stronger chemical interaction between the phenyl sulfonic and hydroxyl groups, which results in a more stable colloidal particle with improved heat conductivity. (Yousefi, Shojaeizadeh, Veysi, & Zinadini, 2012).

Universiti Malaya

1.5.2 Ultrasonic Vibration

This approach is also used to produce a stable, homogeneous nanofluid. This method, like the surface chemical approach, tries to break the surface characteristics of the particles and overcome aggregation in order to generate a stable nanofluid. To avoid agglomeration, the particles were broken down using a Probe Sonicator (X. F. Li et al., 2008).

1.5.3 Addition of Surfactant

This technique is used to improve dispersion and stability. With the addition of a surfactant, the hydrophobic surface characteristic would transform to hydrophilic. It is always important to use the correct amount of surfactant in the mixture because an insufficient amount will result in failure to overcome electrostatic repulsion. (Jiang, Gao, & Sun, 2003). Besides that, there are also some setback for this method:

1. The increment in viscosity value
2. Can't be used effectively for application of fluid with temperature more than 60^0C. As the bond between surfactant and nanoparticles will decrease (Assael,

Metaxa, Arvanitidis, Christofilos, & Lioutas, 2005).

Universiti Malaya

1.6 Nanofluid effective Thermal Conductivity

I. Basefluid Type

II. Nanofluid Temperature

III. Nanoparticles material thermal conductivity

IV. Nanoparticle shape

V. Nanoparticle Size

VI. Nanoparticle Concentration

VII. Additives

VIII. Clustering

IX. Acidity (PH)

X. Nanofluid Temperature

1.7 Nanofluid thermophysical properties

One of the experiments we conducted was to look into the thermophysical properties of nanofluids that had been manufactured. This investigation was carried out using a variety of methods and equipment. The following parameters were measured:

1. Thermal Conductivity
2. Density
3. Viscosity
4. Specific Heat Capacity

Universiti Malaya

1.7.1 Thermal Conductivity

Researchers had a breakthrough where addition of a small number of nanoparticles could result in an increased thermal conductivity of a base fluid. Maxwell and Hamilton theories along with aggregation of particles and Brownian motion were introduced to explain this. There are 4 methods to measure the thermal conductivity of nanofluid.

1. Transient Hot-Wire Method (THWM)
2. Hot Disk Thermal Constants Checker
3. Temperature oscillation technique
4. 3W Omega method

1.8 Objective of Study

- To investigate the well dispersed and stable synthesis of variant nanofluids GAGO(Galic Acid treated with Graphene Oxide) and TiSi(Titanium Silica).
- To investigate the effective use of variant water based nanofluids for heat transfer improvement in different heat exchangers which is Circular and Annular Test.
- To analyze the hydrodynamic properties of the nanofluids with different shape of heat exchangers.
- To analyze the varying thermophysical properties of the water based varying nanofluids.

Universiti Malaya

1.9 Problem statement

Working fluids such as water, ethyl glycol, oil, and many others have been employed since the discovery of the heat exchanger. Unfortunately, the thermal characteristics of these working fluids are extremely low. As a result, heat exchangers are developed on a bigger scale to compensate for the low thermal characteristics. The coils or pipes will be able to hold more working fluids if they are manufactured on a large scale.

However, there is a cost issue to consider. Fabrication of a large scale heat exchanger is impractical due to the high cost of the materials required. Aside from that, assembling and disassembling it would necessitate a significant amount of labour. As a result, it was critical to design a solution to this difficulty.

In comparison to ordinary working fluids, nanofluid has significantly better thermal properties. Because of the improved thermal characteristics, it is possible to fabricate a considerably smaller and more efficient heat exchanger. Recently, numerous studies have been undertaken to fully utilise nanofluid in heat exchangers, as it has not been addressed as an alternative to a decade-long process.

Universiti Malaya

CHAPTER 2 : LITERATURE REVIEW

2.1 Introduction

2.1.1 Graphene Nanoplatelets Suspended in Various Basefluids

The experiment was carried out with the help of a Solar Collector (Flat Plate) and the working fluid was functionalized graphene nanoplatelets (f-GNPs). The four different base fluid was prepared which is Ethylene Glycol (EG), Distilled Water : Ethylene Glycol (70:30), and Distilled Water : Ethylene Glycol (50:50). Effectiveness of the analytical model was verified by Experiment outcomes Via Distilled Water {Alawi *et al* }

Some of the characteristics measured in this experiment are temperatures, power, and mass flow rates. Electron microscopes were used to investigate the physicochemical properties of the changed nanofluids, such as particle sizes, stability, and shape. The increase in collector effectiveness was 12.66 percent, 12.64 percent, and 12.65 percent for Ethylene Glycol , Distilled Water : Ethylene Glycol (70:30), and Distilled Water : Ethylene Glycol (50:50), respectively, at 1.5 kg is a mass flowrate min1 and 0.1 wt percent is mass concentration. {Alawi *et al* }

The results also verified an improvement in the f-GNPs nanofluids heat gain (FR) and heat loss (FRUL) coefficients. There are different types of solar collector , but the flat plate solar collector (FPSC) is the most basic, converting energy via an absorbing plate. An absorbing plate's objective is to improve the absorption level of solar energy by using materials with Black colored coated Appearances{Alawi *et al* }

University Malaya

Heat transfer fluids HTFs convert absorbed solar photons to heat, which is then sent through a network of collecting pipes to the absorbing plate. Absorption through direct contact Solar collectors (DASCs) are a different sort of solar collector in which the radiation is absorbed through the heat carried by fluids rather than the heat collected on the plate's surface. Absorption through direct contact Solar collectors (DASCs) are a solar collector types in which sunlight is collected via fluid heat rather than heat acquired on the plate's surface.. The fundamental literature on GNP suspension in **DW** and **EG** is lacking. {Alawi *et al* }

As a result, this work has two parts: an experimental component and an analytical component. The analytical section examined a wide range of operating conditions on three base fluids, including functionalized graphene nanoplatelets (f-GNPs) weight percentages, flow rates, initial temperatures, and initial rates (of heat). A better knowledge of the influence of these limits will considerably improve the operational efficiency of FPSCs {Alawi *et al* }

Universiti Malaya

2.1.2 TiO2 Nanofluid on heat Transfer in Annular Heat Exchanger

Recently examined heat transfer amendment methods, specifically the impact of geometry (such as micro-channel, mini-channel, tube, etc.) on the heat transfer coefficient for the flow in a sudden enlargement or concentraction of the flow. Steps facing backwards or forwards, or on ribbed channels {Nasiri, *et al* }

Experiment with turbulent heat transfer of air-flow above a vertical forward-facing step. They also investigated the impact of step height on the distribution of the local Nusselt number and discovered that adding the height of step in the reattachment point increases the local Nusselt number. Because of their properties, Nanofluids have recently received a lot of attention in heat transfer research. Nanoparticles have larger surface surfaces than micron-sized particles and have the potential to improve heat transmission{Nasiri, *et al* }

As a result, nanofluids can be employed to create smaller and lighter heat exchangers. investigated the laminar flow of nanofluids containing diverse nanoparticles, for example Copper, Silver, Aluminium oxide, Copper Oxide, and Titanium dioxide, at Reynolds numbers ranging from 200 to 600 in the backward-facing step. {Nasiri, *et al* }

Value of N can still be improved by using significantly lower thermal conductivity TiO2 nanoparticles. Based on explored laminar nanofluid-flow in a backward-facing step on a tiny scale and discovered that when the diameter of the nanoparticles decreases, the Nusselt number increases considerably {Nasiri, *et al* }

Universiti Malaya

The goal of this research is to analyse momentum transfer and heat transfer enhancement in an annular channel with concentration using the SST k-turbulence model and compare the results to prior work in this field. {Nasiri, *et al* }

2.1.2.1 Numerical methods

2.1.2.2 Boundary conditions

The employed boundary conditions in the current numerical simulation ranged from 10,000 to 40,000 Reynolds numbers, contraction ratios of 1-2, heat flow of 6,000 W/m2, and TiO2 content. Volume fractions of nanoparticles of 0.5 percent, 1percent, 1.5 percent, and 2 percent with water as the base fluid. For the entrance pipe's inlet segment, uniform inlet velocity was taken into account. The discharge pipe's outlet segment was subjected to the outlet pressure boundary condition. In the current simulation, an iteration of the SST k- viscous model was used., which provided sufficient solutions for incompressible, steady, and turbulent flow near-wall treatment based on the energy and Reynolds averaged Navier-Stokes equations. {Nasiri, *et al* }

Universiti Malaya

2.1.2.3 Effect of concentration ratio

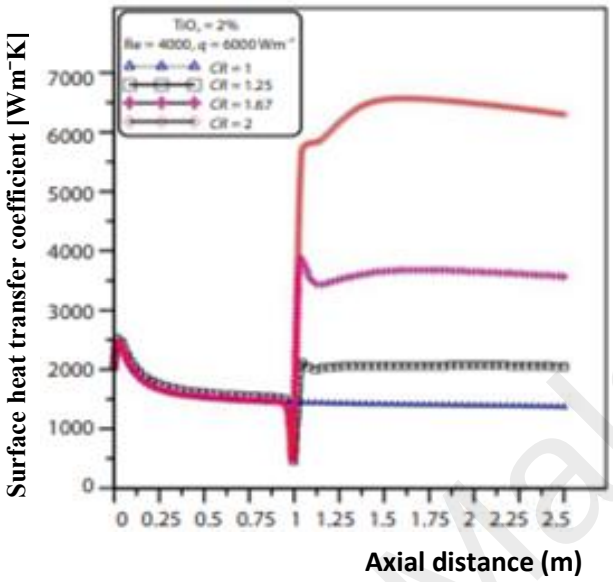

Figure 2.1 above shows the Impact of the concentraction ratio on the external heat transfer coefficient of 2 percent of TiO2 Nano fluid at Re = 40,000 and q = 6,000 W/m². {Nasiri, *et al* }

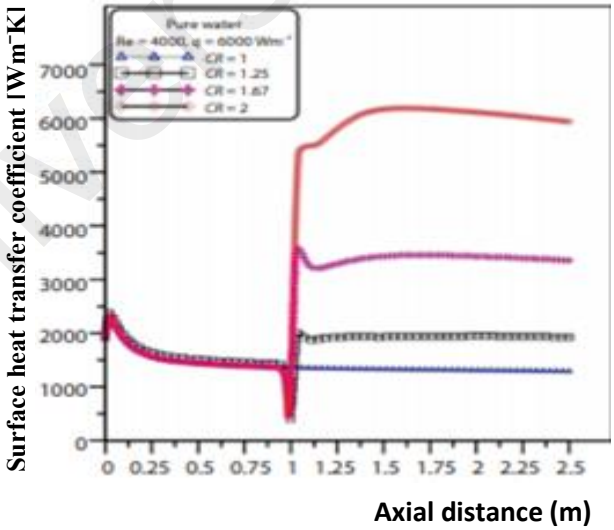

Figure 2.2 above shows the Impact of the concentraction ratio on the external heat transfer coefficient for pure water at Re = 40,000 and q = 6,000 W/m². {Nasiri, *et al* }

Universiti Malaya

Figures 2.1 and 2.2 show the influence of the ratio contration's on the surface heat transfer coefficient for a volume fraction of 2% TiO2 nanoparticles and Distilled water at Re = 40,000 and a heat flow of 6,000 W/m². According to the results of numerical obtained in all circumstances, at the incoming pipe, the surface heat transfer coefficient profile follows the same pattern., although the disparities between heat transfer coefficients. {Nasiri, *et al* }

Universiti Malaya

2.1.2.4 The effect of volume fraction

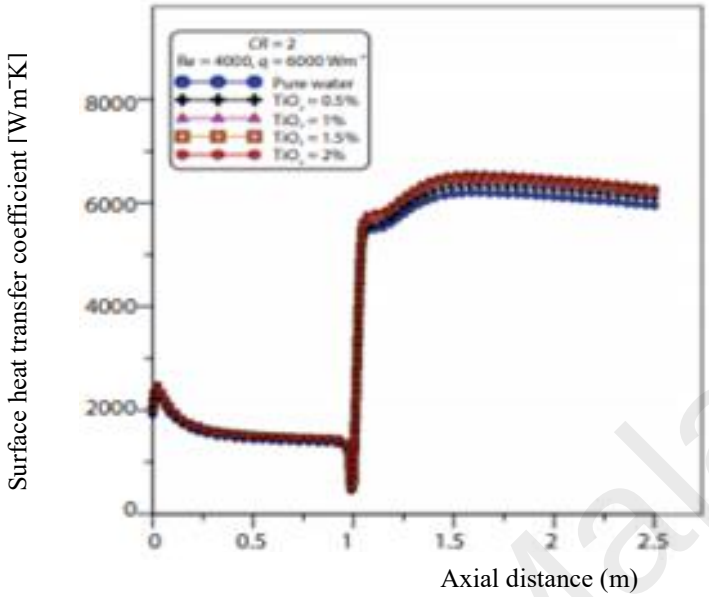

Figure 2.3 shows the heat transfer coefficient of volume fractions Re = 40,000 and CR = 2 at Re = 40,000 and q = 6,000 W/m². {Nasiri, *et al* }

Above graph depicts the surface heat transfer coefficient distribution at various nanoparticle volume fractions (0.5-2 percent), Re = 40,000 and concentraction ratios of 2. In general, rising the nanoparticles's volume of fraction enhances the surface convective heat transfer coefficient in annular pipe flow with flow passage concentraction.. The results show that the interaction of nanoparticle volume fraction with re-circulation flow leads in improved thermal performance. In the previous study, the maximum value of heat transfer coefficient was obtained at a volume fraction of 2 percent TiO2 when compared to others.

Universiti Malaya

2.1.2.5 The effect of heat flux

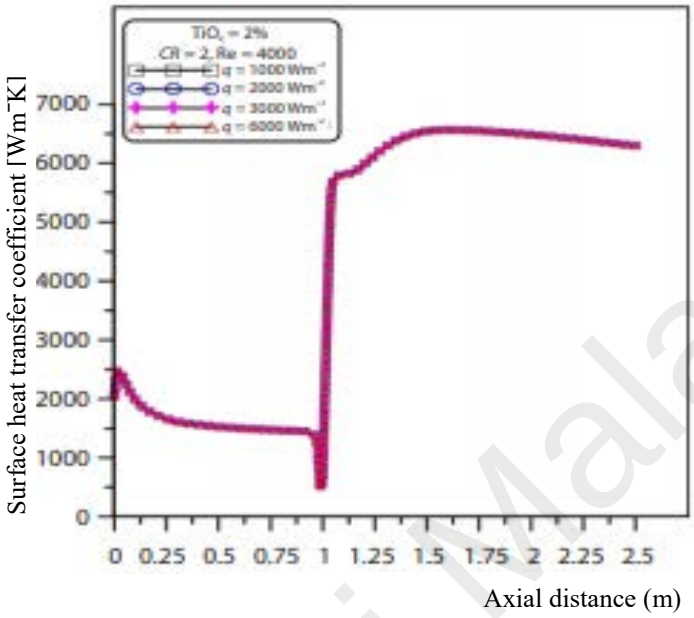

Figure 2.4 above shows the heat flux Impact external heat transfer coefficient of TiO2 at Re = 40,000 and CR = 2 {Nasiri, *et al* }

Above graph depicts the spectrum of surface heat transfer coefficients for a volume fraction of 2 TiO2 nanoparticles at Re = 40,000 and a concentraction ratio of 2percent . As can be seen, there is no discernible rise in surface heat transfer coefficients with increasing heat flux.In this example, heat transfer coefficients follow a similar pattern.

Universiti Malaya

2.1.2.6 Pressure drop

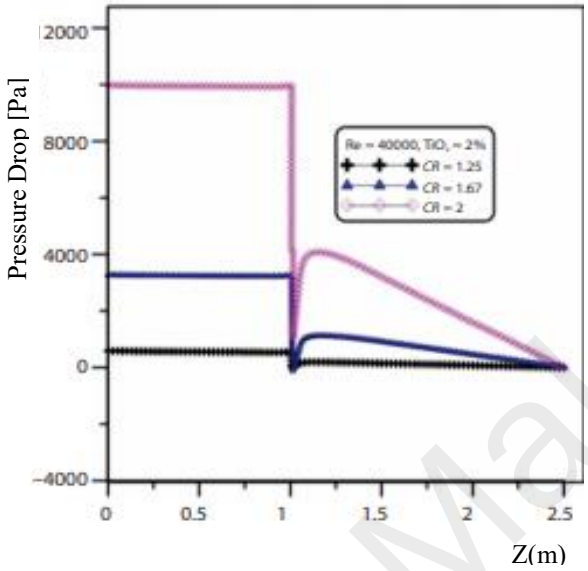

Figure 2.5 above shows the Pressure drop variations for 2 percent TiO2 Nano-fluid at various concentractions proportion. {Nasiri, *et al* }

Above graph depicts pressure drop variations for a 2 percent TiO2 volume fraction suspension at Re = 40,000 and varied contraction ratios. The outcomes reveal that the pressure drops and increases abruptly prior to and following the step, respectively, due to the re-circulation flow caused by hydrodynamic fluid-flow across the channel .

Universiti Malaya

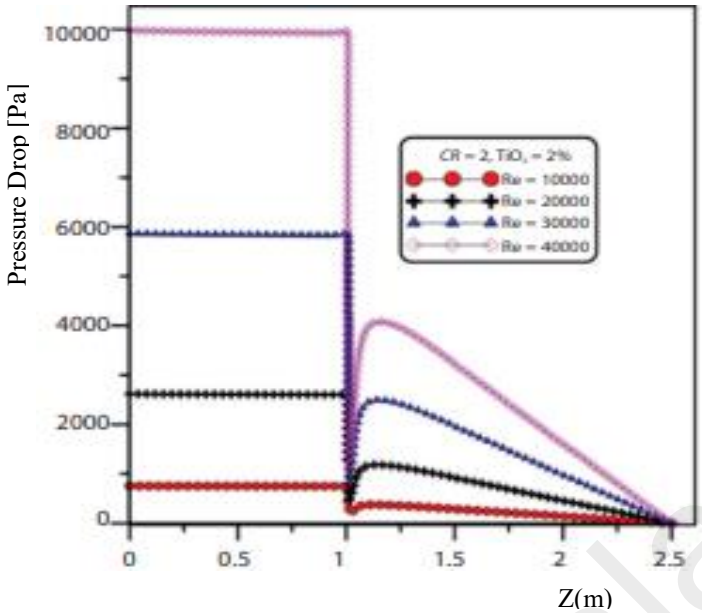

Figure 2.6 above shows the Pressure drop variations for 2 percent of TiO2 nanofluid at various Reynolds numbers. {Nasiri, *et al* }

Above graph depicts the impact of Reynolds number on pressure decrease at 2 percent TiO2 volume fraction and a concentraction ratio of 2. Pressure drop increases as the Reynolds number increases, and the highest value of pressure drop is reached at the maximum value of Re = 40,000 when compared to others in the current range of inquiry.

Universiti Malaya

2.1.2.7 The distribution of velocity

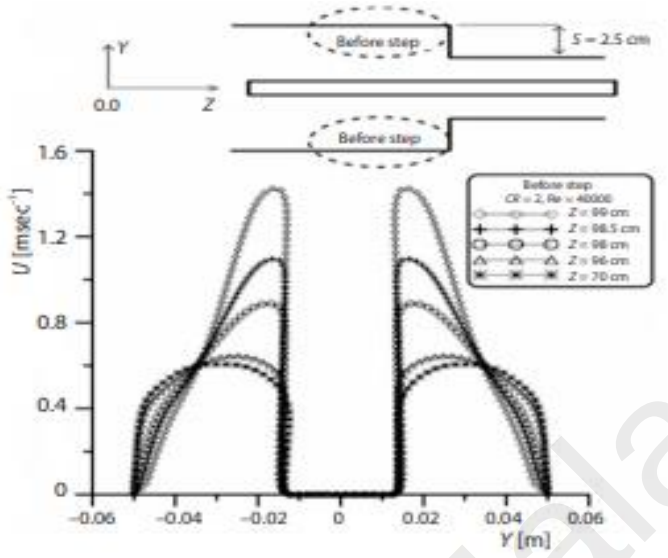

Figure 2.7 Before step, velocity distributions at CR = 2 and Re = 40,000 for various places {Nasiri, *et al* }

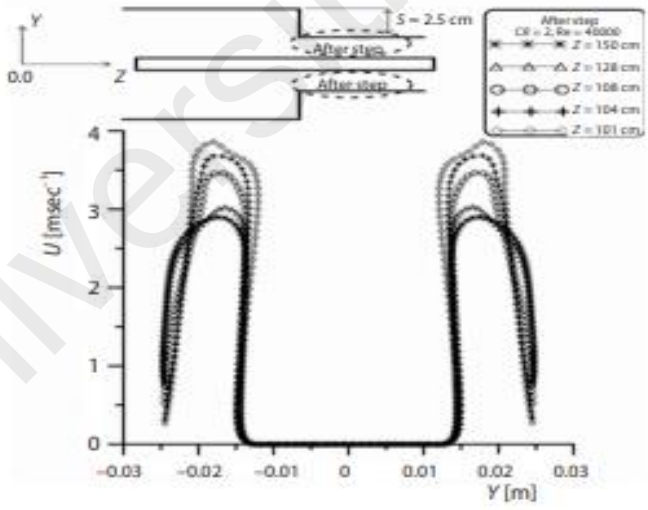

Figure 2.8 Distributions of velocity at CR = 2 and Re = 40000 for various before and after positions {Nasiri, *et al* }

Universiti Malaya

Figures 2.7 and 2.8 depict the velocity distribution before and after the step at Re = 40,000 and a concentration ratio of 2. Before and after the step, the fully developed velocity with 2 circulation zones is observed, with the size of the re-circulation region appearing to decrease with increasing distance from the step. When compared to the other situations, the concentration ratio of 2 had the highest re-circulation flow before and after concentration.

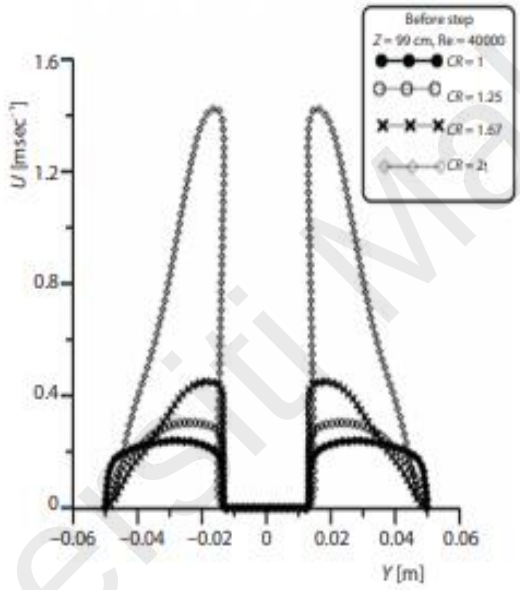

Figure 2.9 The influence of the concentraction ratio on velocity distributions before to the step is shown. at Z = 99 cm for Re = 40,000(Kherbeet *et al*)

Universiti Malaya

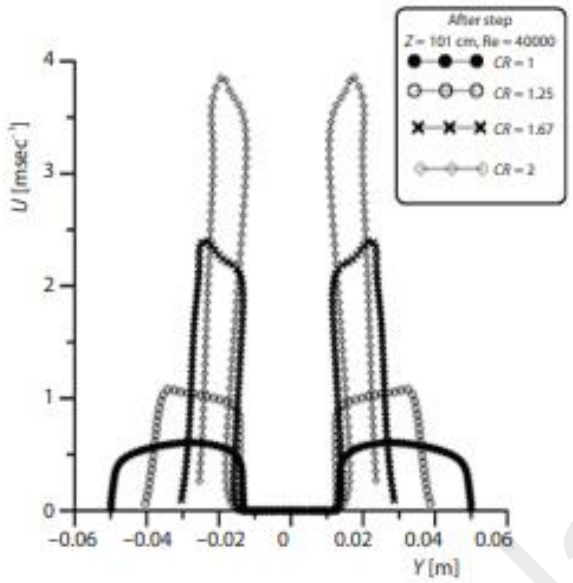

Figure 3.0 Demonstrates the influence of the concentration ratio on velocity distributions after the step at Z = 101 cm for Re = 40000. (Kherbeet *et al*)

Figures 2.9 and 3.0 show the influence of ratio concentraction's on velocity profile at 99 cm before the step and 101 cm after the step for Re = 40000. Because of the re-circulation zones formed before and after the step, the velocity distribution appears to shift as the concentraction ratio increases, affecting the thermal performance.

The influence of the Reynolds number and contraction ratio on surface heat transfer coefficient and heat transfer coefficient increment was explored. In the examined range, the concentraction ratio of 2 resulted in the greatest heat transfer improvement. Heat transfer was improved as a result of the establishment of re-circulation flow before and after the step. In all circumstances, when the Reynolds number and contraction ratio grow, the pressure drop increases, then reduces with the distance before the step and progressively increases after the step.

Universiti Malaya

2.1.3 Numerical simulations of nanofluid convection heat transfer inside closed conduits: a survey

Based on Survey analysis on the effect of Nano-fluids on heat transfer to determine property enhancement as well as flow passage configuration rearrangement the primary goal of this research is to expand it via natural, forced, and mixed methods. For single- and two-phase mixture models, heat transport properties of Nano-fluids are exclusively via convection. By Amending the strength of heat treatment device on energy consumption at the same time reducing the size of such devices, at the end outcome in low material and production cost. {Safaei, *et al* }

Report data on Nano-fluid convection heat transfer and fluid flow via a 10.66-mm diameter tube, specifically, ‘‘dispersed fluid with submicron particles. "The made use of nanoparticles measuring between 13 and 27 nm in size and called the fluids are referred to as Nano-fluids. With an increase in viscosity, there would be a significant drop in frictional pressure. This means that, despite the fact that Nano-fluids have a high heat transfer coefficient, When the coefficient rises, there is a significant drop in pressure. Convection heat transfer applications Heat transfer enhancement versus unwanted resultant pressure loss is always an issue{Safaei, *et al* }

Investigations in a similar test rig to the prior carried out the experimental settings. Inner diameter of tube is 4.57 mm and a length of the tube is 457 mm (i.e. length (100 diameters) was used. An important characteristic The small holdup fluid volume of the employed test loop as well as the use of high-temperature water for heating as opposed to electrical heating. {Safaei, *et al* }

Universiti Malaya

2.1.4 Experimentally, performance of heat transfer and frictional loss of a functionalized GNP-based water coolant in a closed channel flow were examined.

The friction factor and convective heat transfer coefficient of trimethylolpropanetris[poly(propylene glycol), amine terminated] in fully developed turbulent flow Water coolants based on Ether-treated graphene Nanoplatelet (TMP-treated GNP) are found constant velocity at experiment running through a horizontal copper tube with homogenous heat fluxes.. TMP-treated GNP-based water coolant colloidal stability reveals the coolants' high potential for application in heat transfer equipment.. The studies were then carried out over a Re range of 3900–11[thin space (1/6-em)] 700 at constant velocity flow (1–3 m s1) and concentrations ranging from 0.025 to 0.1 with percent.{Yarmand, ***et al*** }

At a heat flow of 23[thin space (1/6-em)]870 W m2, 72 percent of Nusselt number was increased. Nevertheless, the friction aspect drops in the 4–10% level at the same time. The findings imply that TMP-treated GNP-based water coolants have the potential to be effective working fluids in heat transfer applications., offering viable alternatives to standard working fluids{Yarmand, ***et al*** }

The goal of this research is to gain a better knowledge of the relationship between heat transmission and thermo physical parameters in TMP-treated GNP coolants. The thermo physical characteristics of TMP-treated GNP, including heat conductivity and viscosity, were investigated at various concentrations (0.025, 0.05, 0.075, and 0.1 wt percent). {Yarmand, ***et al*** }

Universiti Malaya

The convective of heat transfer coefficient's fluctuation and friction aspect for TMP-treated GNP Nano-fluid are investigated under turbulent flow conditions, which include Nusselt number, pumping power, loop efficiency, and performance index (velocities ranging from 1 to 3 m s1) through a horizontal copper tube at constant heat fluxes of 23[thin space (1/6-em)]. 870 m2 and 18 [thin spacing (1/6-em)] 565 W m{Yarmand, ***et al*** }

Universiti Malaya

2.1.5 Effect of nanofluid thermophysical characteristics on heat transmission and pressure drop.

In this Research study on experimental and computational investigation was carried out to assess when the different type of thermal conductivity Nano-fluids is compared to the effects of momentum and thermal diffusivity on turbulent forced convection heat transfer. {Tiwari, ***et al*** }

This study used 1 percent, 2 percent , and 3 percent volumetric concentrations of different Nano-fluids, including Aluminium Oxide-Distilled water, Silicon dioxide-distilled water, and Copper-Distilled water and their properties were numerically analyzed at a flow input temperature of 30 °C. The experiments were carried out using distilled water as a working fluid. Validate the two-dimensional numerical model. The flow was kept at a Reynolds number between 6,000 and 12,000, and the experimental data were corroborated by empirical correlation results{Tiwari, ***et al*** }

Pressure drop and average Nusselt number of Numerical Solution with the experimental results, with heat transfer and pressure loss statistics have an average inaccuracy of less than 5 percent . The results revealed that Al2O3-DW Nano-fluid had the best boost in convection heat transfer coefficient when compared to DW and other Nano-fluid of the same concentration. While Cu-DW Nano-fluid demonstrated the least enhancement, they also had the maximum degree of thermal conductivity. {Tiwari, ***et al*** }

Universiti Malaya

The experimental research for this work was carried out in the test rig, which comprises of a main flow loop with bypass, pump, flow meter, dpt, valves, pressure gauges, cooler, jacketed tank, thermocouples, power supply, and the test section. The primary component of the exam is a straight a stainless-steel tube with an inner diameter of 10 mm and a total length of 1,400 mm, the heated location of the test section was prepared by carefully rapping the outer surface of the tube up to 1,200 mm length with an electrical tape heating element with a maximum power capacity of 900 W and controlled by a variable voltage transformer. The impact of momentum and thermal diffusivities on nanofluid thermal conductivity on heat transfer and pressure drop in a circular closed conduit flow will be researched experimentally and numerically.{Tiwari, ***et al*** }

Universiti Malaya

2.1.6 The effect of sonochemically synthesized ZnO-water nanofluids on heat transfer in a circular flow channel.

The current study focused on the sonochemical production of ZnO nanoparticles and their good impacts on heat transfer enhancement when utilised as water-based Nanofluids in a circular tube heat exchanger. ZnO nanoparticles were dispersed in distilled water using high probe sonication, and their concentration was varied (0.1 percent, 0.075 percent, 0.05 percent, and 0.025 percent) in order to investigate their effect on convective heat transfer (Nusselt number) with Reynolds number variation in a single tube circular heat exchanger..{Ahmed, *et al* }

High probe sonication was used to distribute ZnO nanoparticles in distilled water., and their concentration was varied (0.1 percent, 0.075 percent, 0.05 percent, and 0.025 percent) in order to investigate their impact on convective heat transfer (Nusselt number) with Reynolds number variation in a single tube circular heat exchanger.{Ahmed, *et al* }

At the highest Reynolds number, there was around 50% heat transfer augmentation at 0.1 percent ZnO Nanofluid concentration (Examined). When compared to the base fluid, all other weight percent concentrations indicated superior heat transfer properties.. The combination of ZnO with distilled water Nanofluids yields encouraging findings for heat transfer enhancements.{Ahmed, *et al* }

The goals of this study are to synthesise ZnO nanoparticles with regulated particle size and spherical form, as well as ZnO-DW Nanofluids with maximum heat transfer, good dispersion, and stability at (0.1, 0.075, 0.05, and 0.025) percent nanoparticles concentrations in distilled water. {Ahmed, *et al* }

Universiti Malaya

The heat transfer coefficient and Nusselt numbers for distilled water Nanofluids at various ZnO-DW concentrations (0.1%, 0.075%, 0.05%, and 0.025%). In the aforementioned investigation, nanofluids were monitored at various points along the circular test section in turbulent flow zones. {Ahmed, *et al* }

Universiti Malaya

CHAPTER 3: METHODOLOGY

This section will cover the setup and preparation required before and after the experimentation and simulation work was completed. Some processes must be performed to ensure that the experimental run produces the intended results.

3.1 Materials and methods

3.1.1 GAGO Composite Nanofluids preperation

This work made use of graphite flakes with 100 meshes (Sigma), potassium permanganate (99 percent), sulphuric acid (95–97 percent), hydrochloric acid (37 percent), diethyl ether, ortho-phosphoric acid (85 percent), and hydrogen peroxide (35 percent) by Riendemann chmidt, gallic acid (97 percent purity) (Sigma-Aldrich), and ethyl alcohol (All of the aqueous solutions were made with deionized water (18.2 M cm). The enhanced Hummers method was used to manufacture graphene oxide from graphite (Gr). A 9:1 concentrated H2SO4/H3PO4 (360:40 mL) mixture was mixed to a graphite flakes (3.0 g, 1 wt equiv) and KMnO4 combination (18.0 g, 6 wt equiv).

After that, reaction was then boiled to 50 °C and stirred for 12 hours.. Before being placed on ice ,(400 mL) with 30% H2O2 (3 mL), the reaction was cooled to room temperature. The resulting suspension was centrifuged at 4000 rpm for 5 minutes before being washed with Volume of DW, HCl (37 percent), AND ethanol is 200 mL, in that order.

The final product was coagulated with 200 mL of diethyl ether before being filtered using an Omnipore TM membrane with 0.2 m pore size.The GO collected on the filter was dried in a 40

Universiti Malaya

°C oven [30]. A 1% pure (GA) solution was dissolved in DIW, and 0.1 g of GO was added, with the pH set at 4.71. After stirring for 16 hours, the mixture was washed with DIW to eliminate any unreacted medication. The GOGA nanocomposite was collected through filtering and dried in a 40 °C oven.

3.1.2 TiSi Composite Nanofluids preparation

The existing study is about TiSi composites based on nanofluids for improving heat transmission in a circular heat exchanger. The TiSi was created using a single pot sonochemical process, and the TiSi was obtained from the chemical supplier business Sigma –Aldrich.. Furthermore, the TiSi composite nanofluids were generated for 0.1 percent mass concentration by combining equal amounts of TiSi in the basefluid (DW). TiSi were physically blended in equal parts (50-50) in base fluid (DW) with matching mass percent concentrations (0.1,0.075,0.050,0.025).

This composite mixture was sonicated for 3 hours in a row to get a well-dispersed and homogeneous dispersion of nanoparticles in base fluid (DW). The investigation was focused on four distinct nanoparticle composite ratios (0.1,0.075,0.05,0.025)mass percent. Furthermore, the presented results demonstrate the well-dispersed and suspended TiSi in the base fluid (DW).

Following that, the dilution process is initiated using Equations (1) and (2), where V1 and V2 are documented to verbalise the nanofluid samples at different mixing percentages and 0.1 percent mass concentration.

Universiti Malaya

$$\emptyset = \frac{\omega pbf}{\left(1-\frac{\omega}{100}\right)pp+\frac{\omega}{100}*pbf}$$ Equation 1

$$\triangle V = (V2 - V1) = V1(\frac{\emptyset 1}{\emptyset 2} - 1)$$ Equation 2

The functionalized was then centrifuged to separate the denser nanoparticles. It was also washed several times until the pH value reached neutral. Finally, the functionalized GNP is dried overnight in a 50°C oven. The phenolic acid GNPs were produced at concentrations of 0.1, 0.05, and 0.0025 percent. The flow of phenolic acid functionalized GNP is depicted in the figure below (Sadri et al., 2017).

Figure 3.1 The functionalization method for GAGO

Universiti Malaya

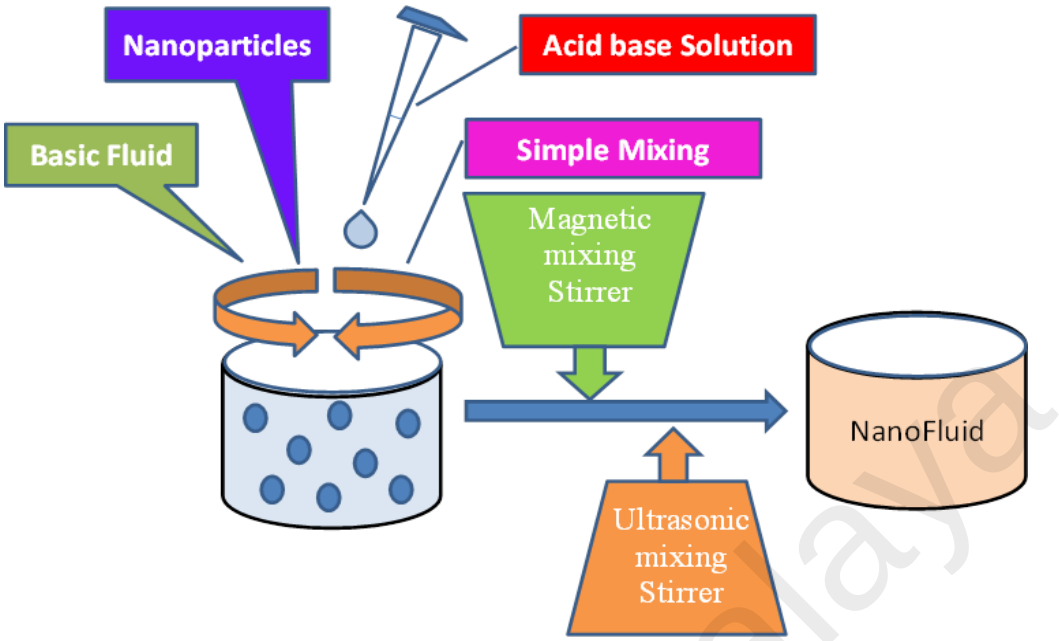

Figure 3.2 The Nanofluid preparation Procedure.

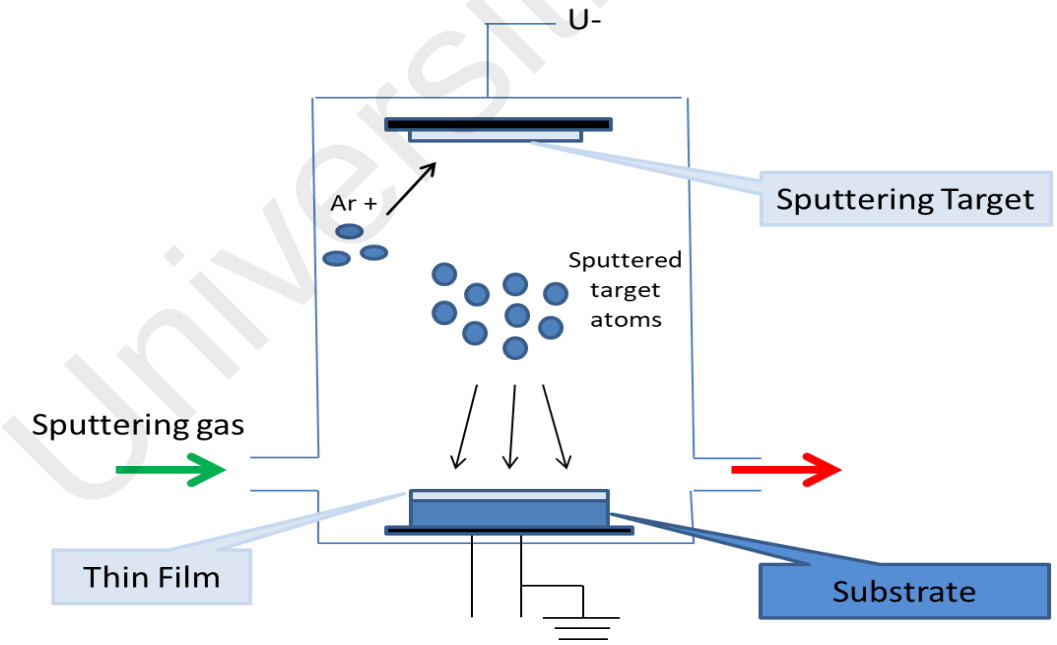

Figure 3.3 Physical Vapour Deposition Method.

Universiti Malaya

3.2 Experimental Set Up

The experiment rig was built in the University of Malaya's CFD Lab. The rig is made up of numerous mechanical and electronic components for data observation and gathering. Figure 3.1 depicts a schematic illustration of the thesis' experimental setup. The setup contains a heater, flow loop connections, a chiller for cooling, and a data logger for data collecting. Figure 3.2 is a snapshot of the rig used in the study, which was set up in the lab.

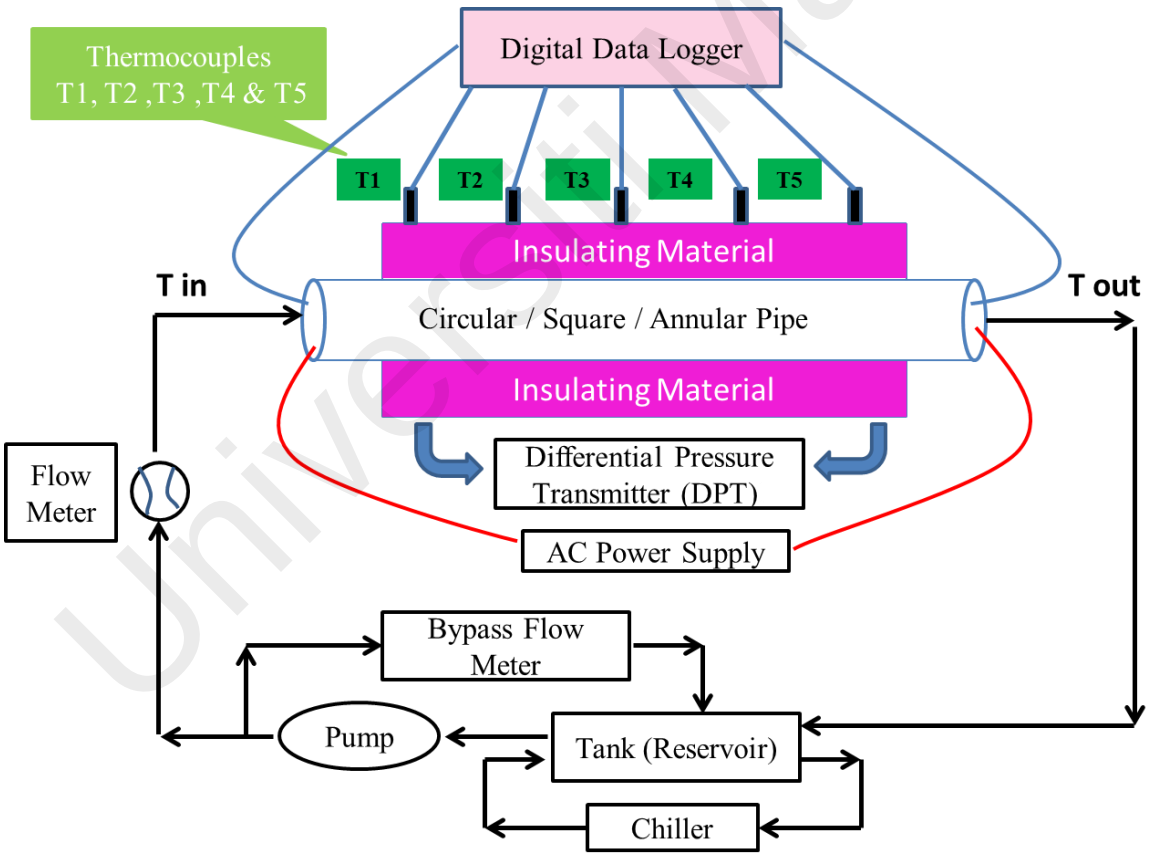

Figure 3.4: The experimental setup rig is depicted schematically.

University of Malaya

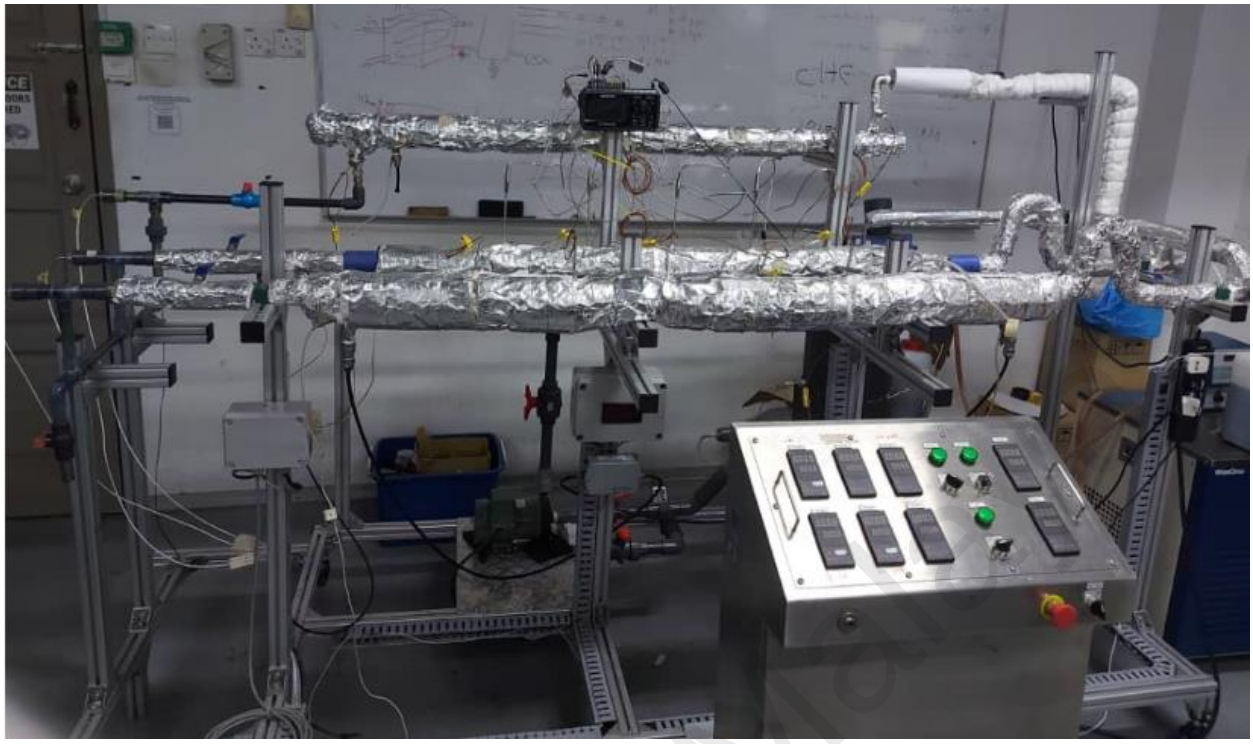

Figure 3.5: Picture of the Rig that experiment conducted

Figure 3.6: Picture of the Rig Control Panel

The rig's flow loop is consists of a reservoir, chiller, pump, and flow rate metre. During experimental runs, the nanofluids are stored in the reservoir, also known as the tank. To prevent nanoparticles from settling, a mechanical stirrer is installed in the tank to ensure a continual movement throughout the fluid. The stirrer was set to a constant revolution of 600 rpm. The reservoir has a tank capacity of 14 litres in total. Only 7 litres of either distilled water or nanofluid are utilised in the investigation.

Futhermore,The chiller is linked to the system to stimulate the operation of a heat exchanger. Throughout the test, the chiller temperature was kept at 20 degrees Celsius. Because the nanofluids absorb heat from the surface of the circular or square pipe, the absorbed heat must be evacuated to prevent the system from overheating. Aside from that, the chiller aids in the creation of a steady state condition to avoid temperature data fluctuation.

Meanwhile, one of the most important components is the pump, which serves to pump the working fluid across the pipeline, where it is circulated through the test section and then released back to the reservoir. To examine the pressure drop across the circular and Annular test portions, a Differential Pressure Transducer (DPT) is placed to the rig on opposing ends. The pressure decrease across the tubes is indicated by a digital metre linked to the transducer. The friction factor of the nanofluids was determined using DPT.

This study was carried out on two separate channels or tubes .One is a circular, and the other is a Annular. The round tube's inner and outer diameters are 10 mm and 12.8 mm, respectively. The inner and outer widths of each cross sectional side of the Annular section are 10mm and 12.8mm, respectively. Both the circular and Annular test sections have a length of 1.2 metres.

Universiti Malaya

The entire surface of the test parts and heater is wrapped. The heater produces a steady heat flux on the wall border using power supplied from the mains via a transformer. The thermocouple is put on the test portions at varied intervals, as specified and seen in both the schematic and image. The thermocouple's purpose is to record temperature on the wall at regular intervals.

Meanwhile, the thermocouple put into the nanofluid flow stream records the input and output temperatures. T-type thermocouples are employed in all of the setup's thermocouples. These thermocouples are sensitive at low temperatures, which is ideal for the application.

3.2.1 The Digital Data logger

The test channels surface temperature is recorded using a Graphtec digital Logger GL220, as shown in Figure 3.4. The thermocouples were all connected to the logger, and the temperature rise and fall were observed in real time. As there are 10 input channels available, a total of 10 thermocouples can be connected to the logger.

The Burkert Electromagnetic Flow Meter, like the flow rate metre, is used to continuously monitor and control the flow measurement of the working fluid. In addition, a pressure transducer is installed on the test channel at the outlet and inlet to allow the DPT to read the pressure decrease across the rig.

Universiti Malaya

Figure 3.7: The Digital data Logger GL220

3.2.2 The Test channel

The test section on which the trial runs were carried out was made of stainless steel and had the dimensions specified previously. Grooves were prepared on the surface of the tube to accommodate the thermocouples, and it was ensured that the holes were not hollow to prevent the thermocouple from coming into direct contact with the fluid flowing through the tube, as the goal was to record the surface temperature rather than the fluid temperature. On the test part, a holder-like structure with a slot was placed. To attach the holder at the grooved places, epoxy was utilised as an adhesive. Thermocouples were then fully put into the slot until they made contact with the test section's surface.

Universiti Ma

3.3 Data processing

The sections that follow create and process the experimental data used to assess the hydrodynamic and heat transfer performance of GAGNP-water nano-coolants flowing through a closed conduit. To eliminate boundary layer disruption caused by thermocouple probes poking into the tube's interior surface, the thermocouples were put on the tube's outer surface. Calibration was required to ascertain the temperatures at the internal tube surface due to conduction in the tube wall and convection heat transfer with the fluid at the test section. As a result, an analysis based on the Wilson plot approach was performed, which involved equating the resistance between various portions in the heat transmission direction's and monitoring the temperature of the horizontal pipe's inner surface through mathematical manipulation. The heat transfer coefficient (h), the Nusselt number (Nu), and the pressure drop (DP) are relevant metrics to investigate the effect of GA-treated GNPs on the thermal characteristics of distilled water. The experimental heat transfer coefficient was calculated using Newton's cooling equation and the *measured surface, bulk, outlet*, and *input temperatures*.

$$h = \frac{q''}{(\mathrm{T}w - \mathrm{T}b)} \qquad \text{Equation 1}$$

where T*b*, T*w*, and q^{n} are the bulk, wall, and heat flux temperatures, respectively. T*b* is defined as $\frac{To+Ti}{2}$, where T*i* and T*o* are the input and output flow temperatures. The heat flux can be computed using the formula,

Universiti Malaya

$$q^{"} = \frac{Q}{A}$$ Equation 2

where Q is the power supply's input power (VI), and A is the heated inner surface area of the tube A = pDL in this case. In this experiment, an input power (VI) of 600 W was employed.The non-dimensional heat transfer coefficient is specified as the Nusselt number, which is defined as:

$$Nu = \frac{h \times D}{K}$$ Equation 3

where K, h, and D are the thermal conductivity, convective heat transfer coefficient, and inner diameter of the tube, respectively. Gnielinsky [48], Petukhov [49], and Dittuse Boelter [50] proposed empirical correlations for Nusselt number for single-phase fluids, respectively.

$$Nu = \frac{(\frac{f}{8})(Re-1000)Pr}{1+12.7\left(\frac{f}{8}\right)^{0.5}(Pr^{\frac{2}{3}}-1)}$$ Equation 4

The Reynolds number is Re, the Prandlt number is Prandlt, and the friction factor is f. In the region of 3 x 10^3 < Re <5 x 10^6 and 0.5 <Pr< 2000, Eq. (4) is employed.

$$Nu = \frac{(\frac{f}{8})RePr}{1.07+12.7\left(\frac{f}{8}\right)^{0.5}(Pr^{\frac{2}{3}}-1)}$$ Equation 5

Universiti Malaya

Eq. (5) is valid for values between 10^4 < Re < 5x10 ^{6} and 0.5 ≤ Pr ≤2000.

$$Nu = 0.023Re^{0.8}Pr^{0.4} \quad \text{Equation 6}$$

In the range of Re > 104 and 0.7 Pr 160, Eq. (6) is utilised. In Eqs. (4) and (5), the friction factor, f, is provided as Petukhov. [49]

$$f = (0.79LnRe - 1.64)^{-2} \quad \text{Equation 7}$$

In the range of 10^4 Re 10^6, Eq. (7) is utilised. Using the experimentally recorded pressure drop data across the test portion, the friction factor of distilled water and nanofluids was calculated.

$$f = \frac{\triangle P}{(\frac{L}{D})(\frac{pv^2}{2})} \quad \text{Equation 8}$$

Eqs. (7) and (9), respectively, give the empirical correlation utilised to derive the friction factor of the base fluid proposed by Petukhov [49] and Balsius [51].

$$f = 0.3164Re^{-0.25} \quad \text{Equation 9}$$

For the Reynolds number range, 3000 <Re <10^5

The uncertainty values of the collected data, which include the Nusselt number, heat transfer coefficient, friction factor, and Reynolds number, are estimated using the procedures developed

Universiti Malaya

by Kline and Mcclintock [52] and Taylor and Thompson [53]. The following correlation is used to assess the uncertainty of parameter R:

$$U_{\mathrm{r}} = \sqrt{\sum_{i=1}^{n} \left(\frac{\partial R}{\partial V_{\mathrm{i}}} U_{\mathrm{vi}}\right)^2} \quad \text{Equation 10}$$

where U_v and U_r are the uncertainty associated with the independent variable Vi and the parameter R. Furthermore, n is the number of variables that are independent The uncertainty values determined by Eq. (10)

Universiti Malaya

CHAPTER 4: RESULTS AND DISCUSSION

The results of the study's experimental and simulation runs will be carefully detailed in this chapter. To facilitate comparative studies, the results of both the experimental and simulation studies will be given in a graphical format. The nanofluid concentrations evaluated in the paper are 0.025 percent, 0.05 percent, 0.075 percent and 0.1 percent. The type of Nanofluid that being used in this experiment were GAGO/ DW and TiO2+SiO2/DW .The varied nanofluid concentrations are evaluated on the circular and Annular test sections. Comparison of heat transfer improvement of both circular and annular test section for both GAGO/DW and TiO2+SiO2/DW based Nano-fluids.

4.1 Circular and Annular Geometry

The surface area of both the circular and Annular geometries is different. This would have an impact on the total heat transfer process. The temperature, heat transfer coefficient, and Nusselt number at local sites are further explored. The following section will compare the thermal conductivity, temperature, heat transfer coefficient, and Nusselt number of GAGO and Ti Si.

Universiti Malaya

4.1.1 Thermophysical Properties

Thermal conductivity, as the title implies, refers to a solution's or material's capacity to transport heat. This was one of the motivating factors for researchers to investigate the influence of nanoparticles on thermal conductivity when added to a base fluid. Thermal conductivity is affected by elements such as particle volume fraction, temperature, base fluid nature, particle material type, and others. Furthermore, several methods for increasing the thermal conductivity of Nano-fluids have been investigated. The investigations undertaken by researchers in an effort to improve thermal conductivity are included in the following section.

4.1.2 Thermal Conductivity Of GAGO

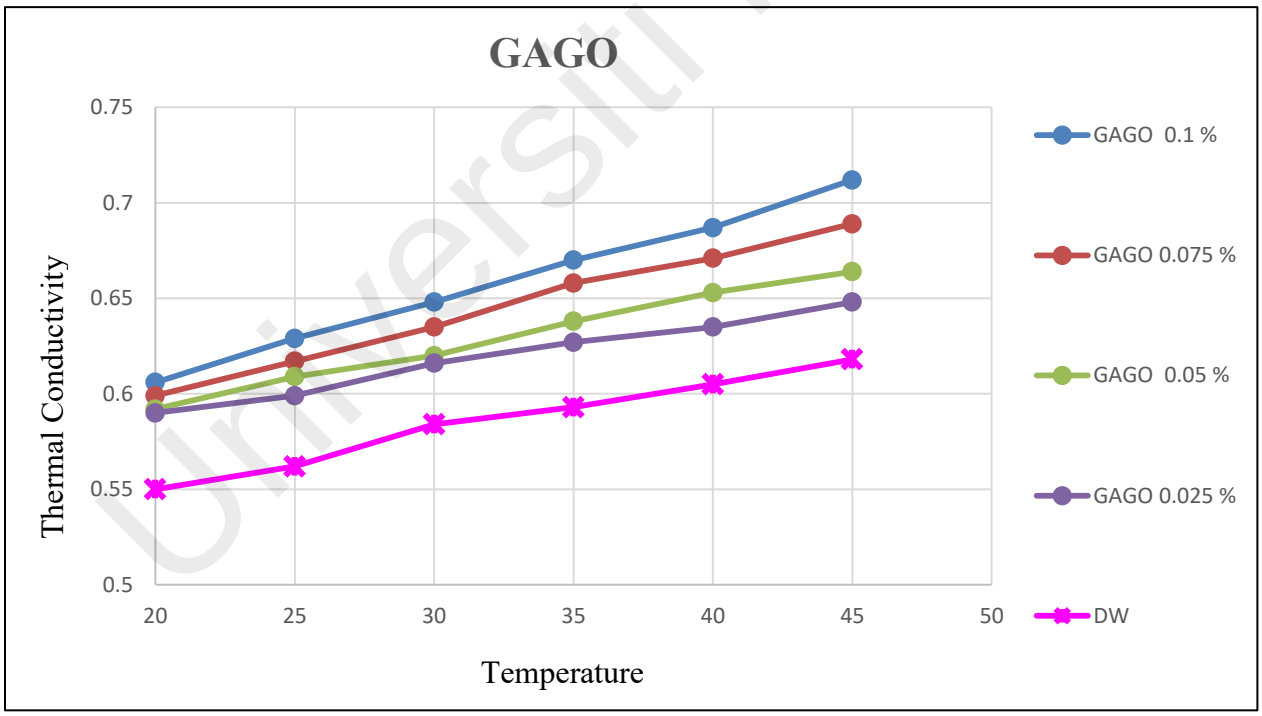

Figure 4.1: Graph of GAGO Thermal Conductivity with DW, 0.025 %, 0.050 % , 0.075% and 0.1%

Universiti Malaya

4.1.3 Thermal Conductivity of TiO2+SiO2

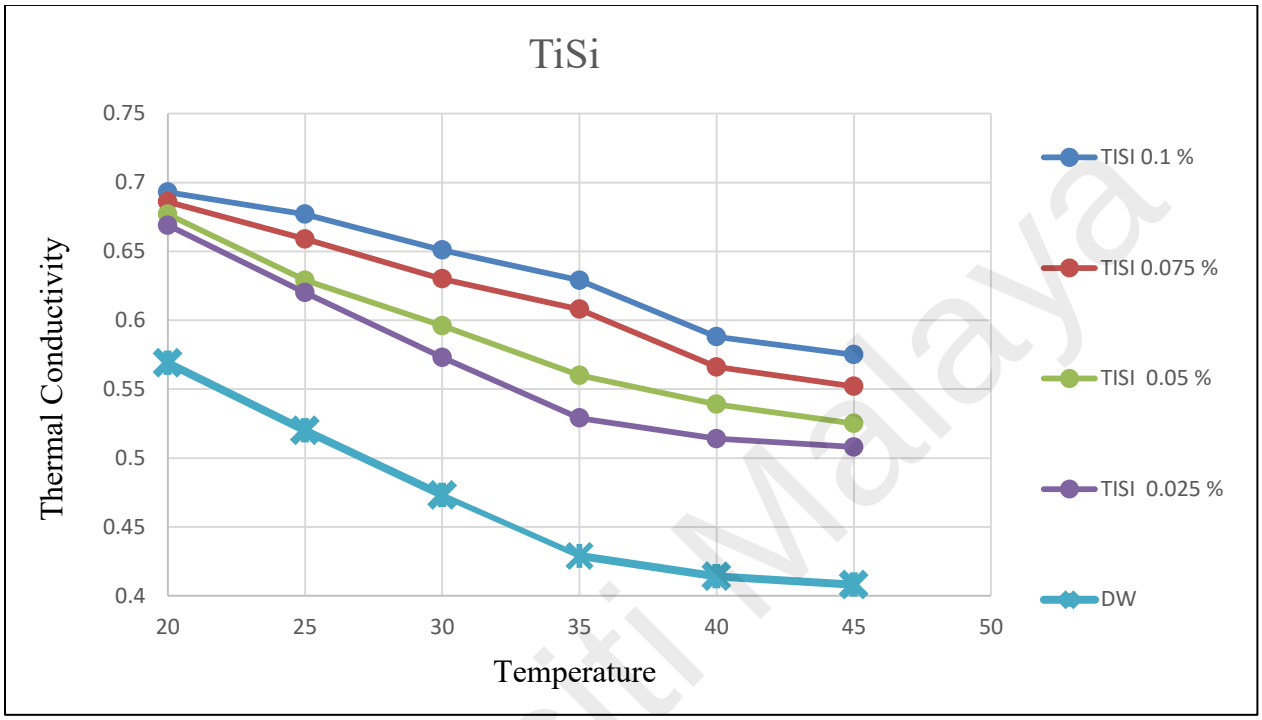

Figure 4.2: Graph of TiSi Thermal Conductivity with DW, 0.025 %, 0.050 % , 0.075% and 0.1%

Universiti Malaya

4.2 Hydrodynamic Properties

4.2.1 Pressure Drop in Circular and Annular Test Section

4.2.1.1 GAGO Pressure Drop Result in Circular Section

GAGO Pressure Drop (Circular)					
Reynolds	GAGO/DW 0.1wt%	GAGO/DW 0.075wt%	GAGO/DW 0.05wt%	GAGO/DW 0.025wt%	DW
13104.4943	1988.8	1838.0	1460.20	1220.50	1041.803
16405.1179	2472.9	2380.0	2052.40	1831.60	1639.300
19703.7414	3144.7	2890.0	2598.00	2445.30	2252.930
23204.3650	3821.5	3681.8	3425.60	3130.60	2913.192
26504.9886	4479.2	4272.5	4153.60	3945.60	3707.403
29805.6122	5428.3	5242.9	5151.50	4835.00	4578.197
33206.2357	6448.4	6331.8	6170.50	5945.00	5730.000

Table 4-1: Table of GAGO Pressure Drop with DW, 0.025 %, 0.050 % , 0.075% and 0.1% In Circular Test Section

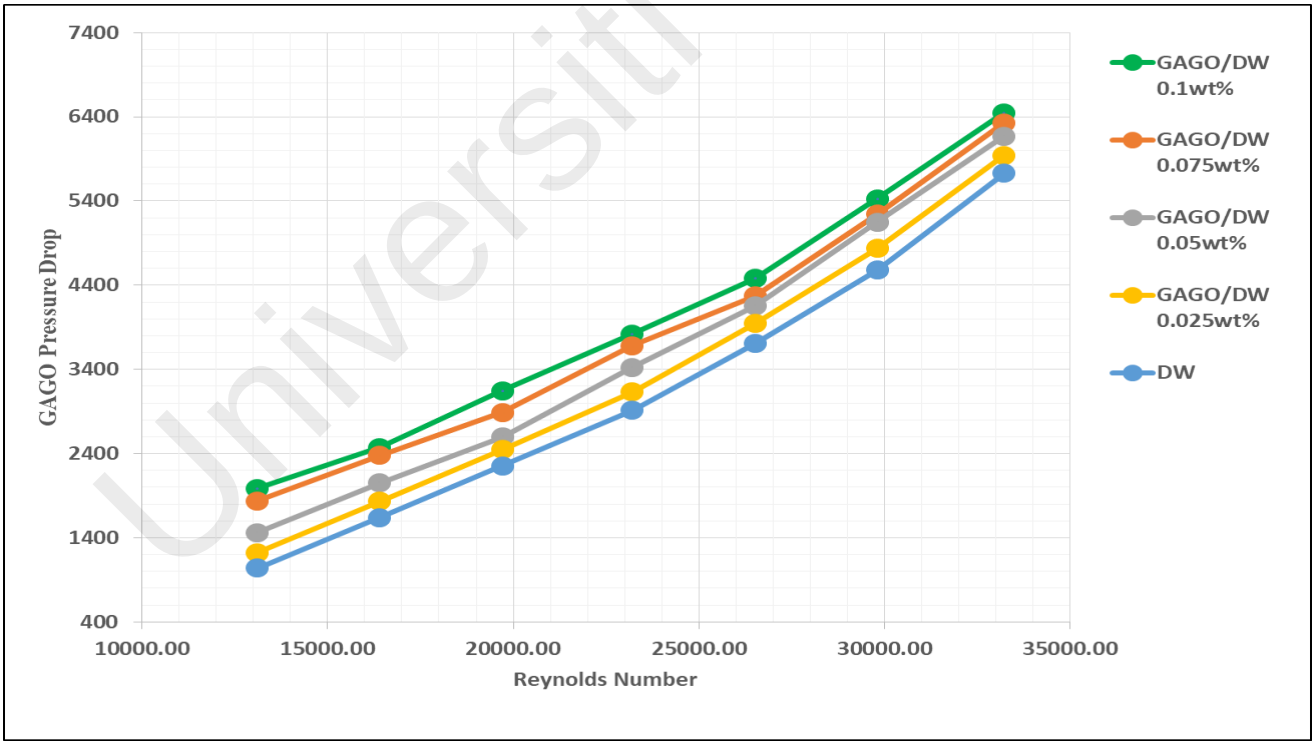

Figure 4.3: Graph of GAGO Pressure Drop with DW, 0.025 %, 0.050 % , 0.075% and 0.1% In Circular Test Section

Universiti Malaya

4.2.1.2 GAGO Pressure Drop Result in Annular Section

GAGO Pressure Drop (Annular)					
Reynolds	GAGO/DW 0.1wt%	GAGO/DW 0.075wt%	GAGO/DW 0.05wt%	GAGO/DW 0.025wt%	DW
3162.0658	112.110	95.844	82.200	76.900	68.995
3955.5822	155.980	143.031	127.250	111.076	97.454
4747.0987	215.905	201.736	181.947	155.051	132.759
5543.6151	276.536	254.282	233.334	202.700	176.269
6330.1316	315.900	293.500	273.300	243.000	218.197
7125.6480	352.700	328.500	304.900	282.000	266.828
7917.1644	398.200	378.800	361.400	341.400	321.820

Table 4-2: Table of GAGO Pressure Drop with DW, 0.025 %, 0.050 % , 0.075% and 0.1% In Annular Test Section

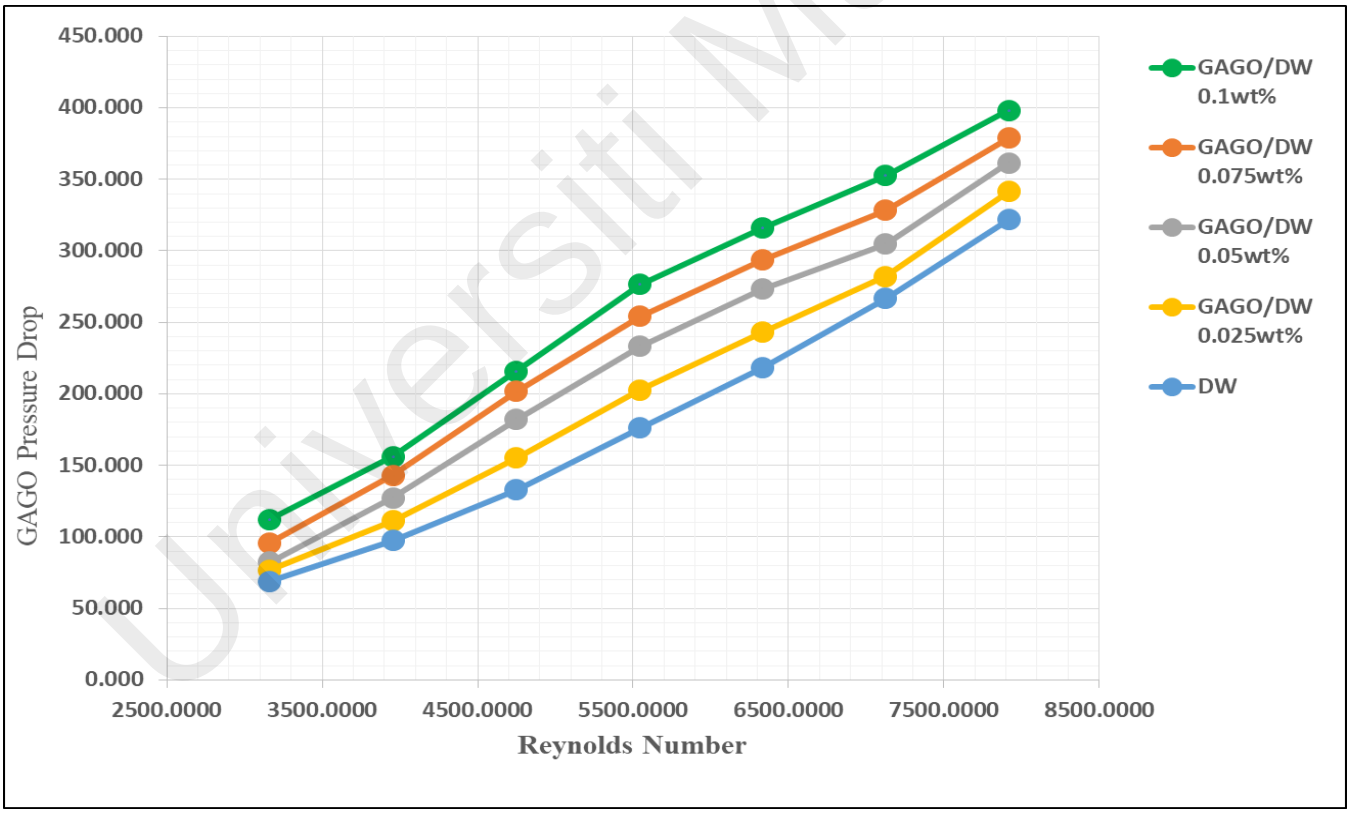

Figure 4.4: Graph of GAGO Pressure Drop with DW, 0.025 %, 0.050 % , 0.075% and 0.1% In Annular Test Section

Universiti Malaya

4.2.1.3 Tisi Pressure Drop Result in Circular Section

TiSi Pressure Drop (Circular)					
Reynolds	TiSi/DW 0.1wt%	TiSi/DW 0.075wt%	TiSi/DW 0.05wt%	TiSi/DW 0.025wt%	DW
13202.49429	1995.9	1753.0	1520.00	1310.90	1150.900
16503.11786	2427.2	2249.0	2043.00	1815.60	1645.600
19803.74144	3089.3	2847.0	2642.40	2468.00	2245.000
23104.36501	3811.8	3555.0	3250.20	3036.00	2840.000
26404.98858	4604.6	4343.0	4122.30	4005.00	3695.000
29705.61216	5625.8	5362.0	5115.90	4886.00	4560.000
33006.23573	6630.2	6507.9	6380.00	6135.00	5830.000

Table 4-3: Table of TiSi Pressure Drop with DW, 0.025 %, 0.050 % , 0.075% and 0.1% In Circular Test Section

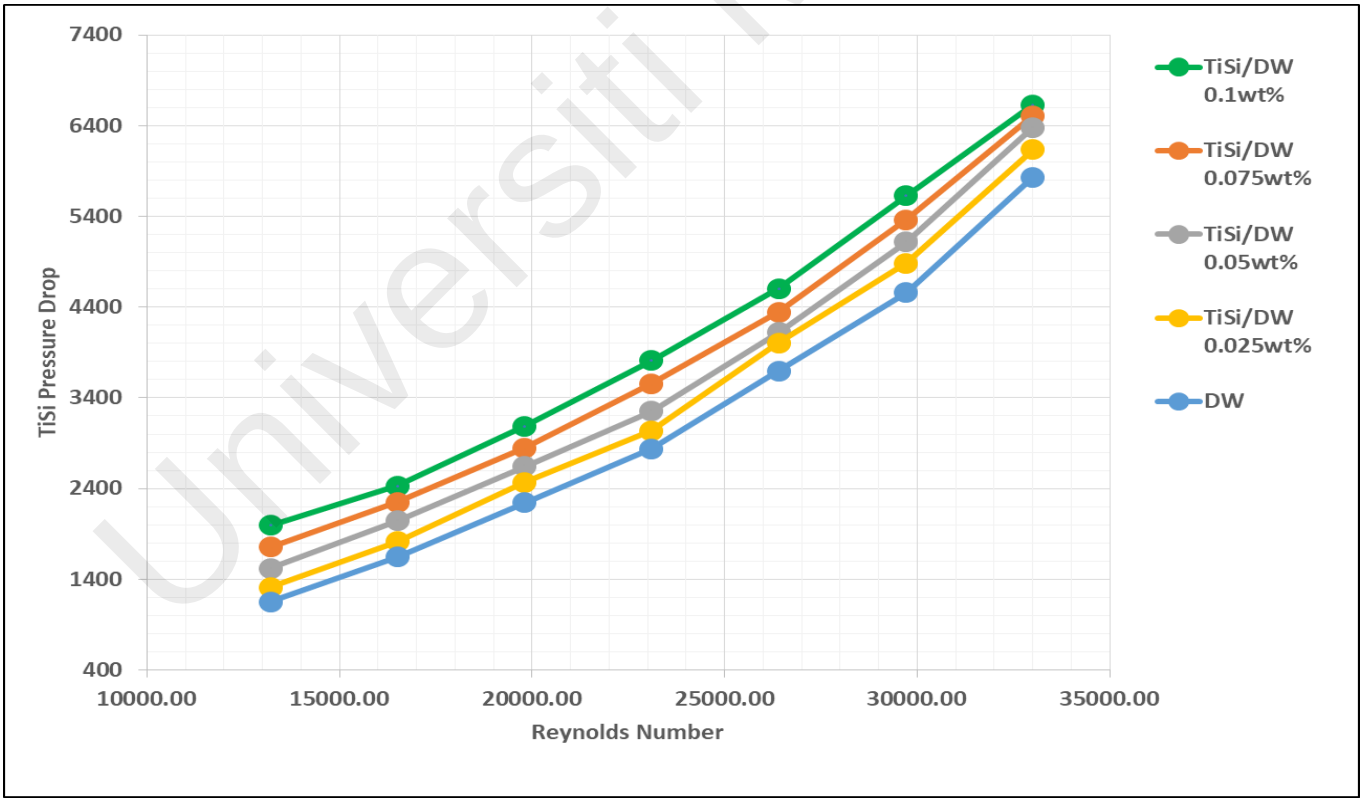

Figure 4.5: Graph of TiSi Pressure Drop with DW, 0.025 %, 0.050 % , 0.075% and 0.1% In Circular Test Section

Universiti Malaya

4.2.1.4 Tisi Pressure Drop Result in Annular Section

TiSi Pressure Drop (Annular)					
Reynolds	TiSi/DW 0.1wt%	TiSi/DW 0.075wt%	TiSi/DW 0.05wt%	TiSi/DW 0.025wt%	DW
3166.0658	96.000	82.000	73.700	64.500	58.300
3957.5822	108.320	94.500	86.200	76.400	71.300
4749.0987	121.600	112.800	99.600	92.400	85.400
5540.6151	136.300	126.100	116.600	107.800	98.400
6332.1316	149.600	143.600	133.600	126.800	117.500
7123.6480	161.500	155.400	145.800	136.500	128.700
7915.1644	171.400	166.600	152.800	141.100	132.700

Table 4-4: Table of TiSi Pressure Drop with DW, 0.025 %, 0.050 % , 0.075% and 0.1% In Annular Test Section

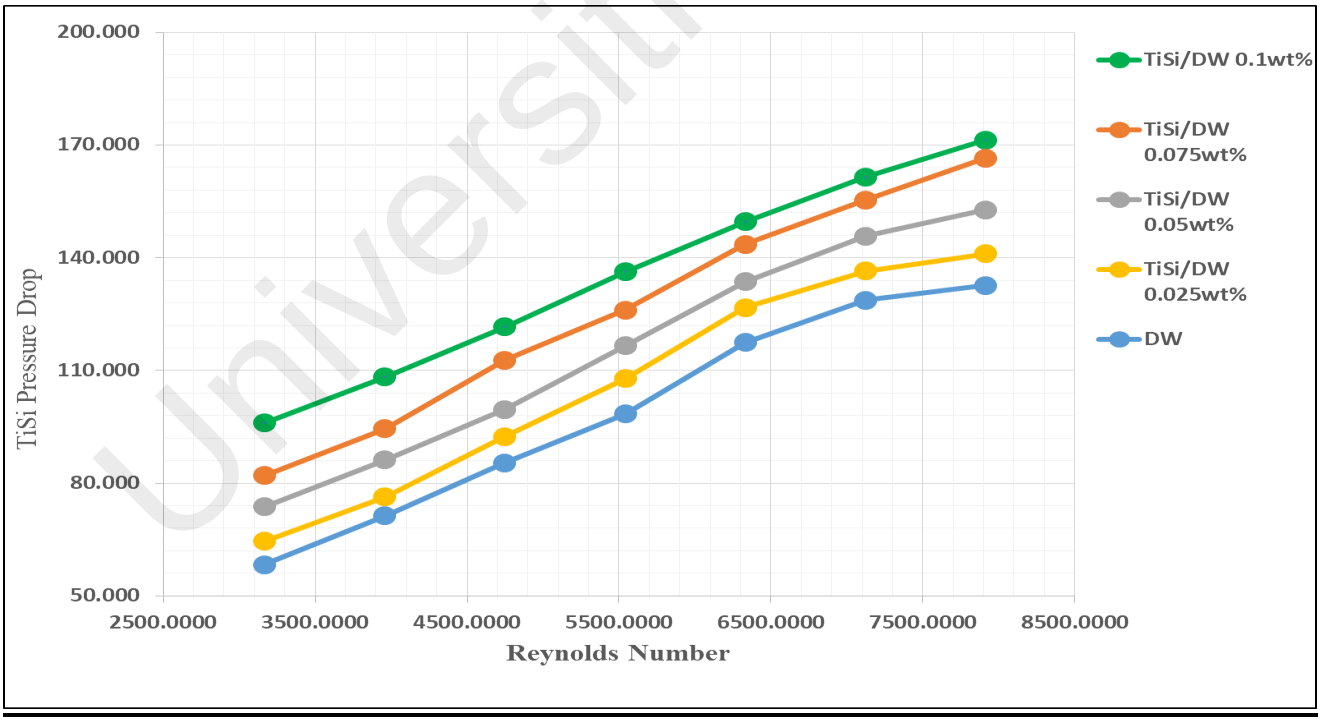

Figure 4.6: Graph of TiSi Pressure Drop with DW, 0.025 %, 0.050 % , 0.075% and 0.1% In Annular Test Section

Universiti Malaya

4.2.2 Friction Loss in Circular and Annular Test Section

4.2.2.1 GAGO Friction Loss Result in Circular Section

GAGO Friction Loss (Circular)					
Reynolds	GAGO/DW 0.1wt%	GAGO/DW 0.075wt%	GAGO/DW 0.05wt%	GAGO/DW 0.025wt%	DW
13244.4943	0.037055	0.035324	0.033327	0.031174	0.0291
16514.1179	0.033938	0.031816	0.029734	0.026900	0.0258
19833.7414	0.029715	0.028017	0.026728	0.025040	0.0239
23123.3650	0.027679	0.026378	0.025119	0.023323	0.0224
26439.9886	0.025879	0.024622	0.023472	0.022350	0.0213
29729.6122	0.024282	0.023432	0.022105	0.021072	0.0205
33098.2357	0.023121	0.022763	0.021609	0.020984	0.0200

Table 4-5: Table of GAGO Friction Loss with DW, 0.025 %, 0.050 % , 0.075% and 0.1% In Circular Test Section

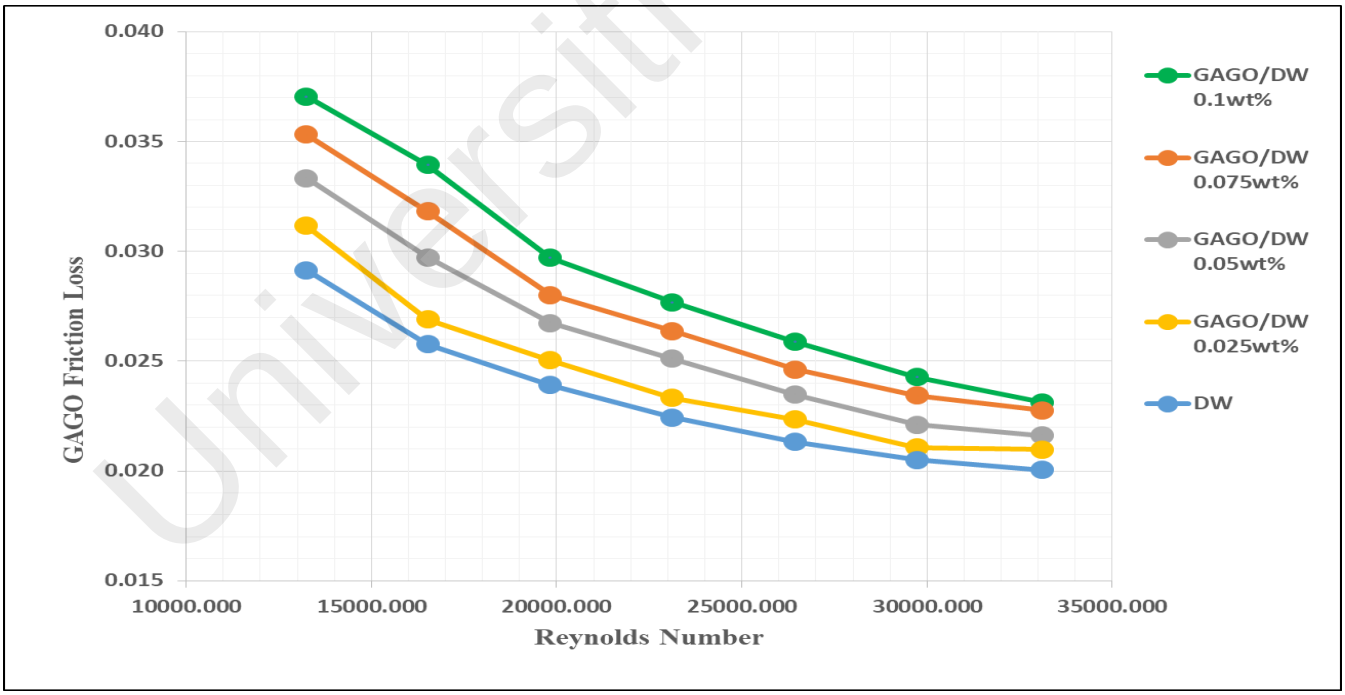

Figure 4.7: Graph of GAGO Friction Loss with DW, 0.025 %, 0.050 % , 0.075% and 0.1% In Circular Test Section

Universiti Malaya

4.2.2.2 GAGO Friction Loss Result in Annular Section

GAGO Friction Loss (Annular)					
Reynolds	GAGO/DW 0.1wt%	GAGO/DW 0.075wt%	GAGO/DW 0.05wt%	GAGO/DW 0.025wt%	DW
3164.0658	0.05463	0.05158	0.04947	0.04604	0.04494
3959.5822	0.04978	0.04774	0.04521	0.04352	0.04172
4747.0987	0.04942	0.04665	0.04367	0.04124	0.03970
5542.6151	0.04656	0.04444	0.04244	0.03987	0.03798
6331.1316	0.04322	0.04102	0.03976	0.03796	0.03592
7125.6480	0.04189	0.03950	0.03749	0.03459	0.03280
7917.1644	0.03907	0.03727	0.03543	0.03247	0.03017

Table 4-6: Table of GAGO Friction Loss with DW, 0.025 %, 0.050 % , 0.075% and 0.1% In Annular Test Section

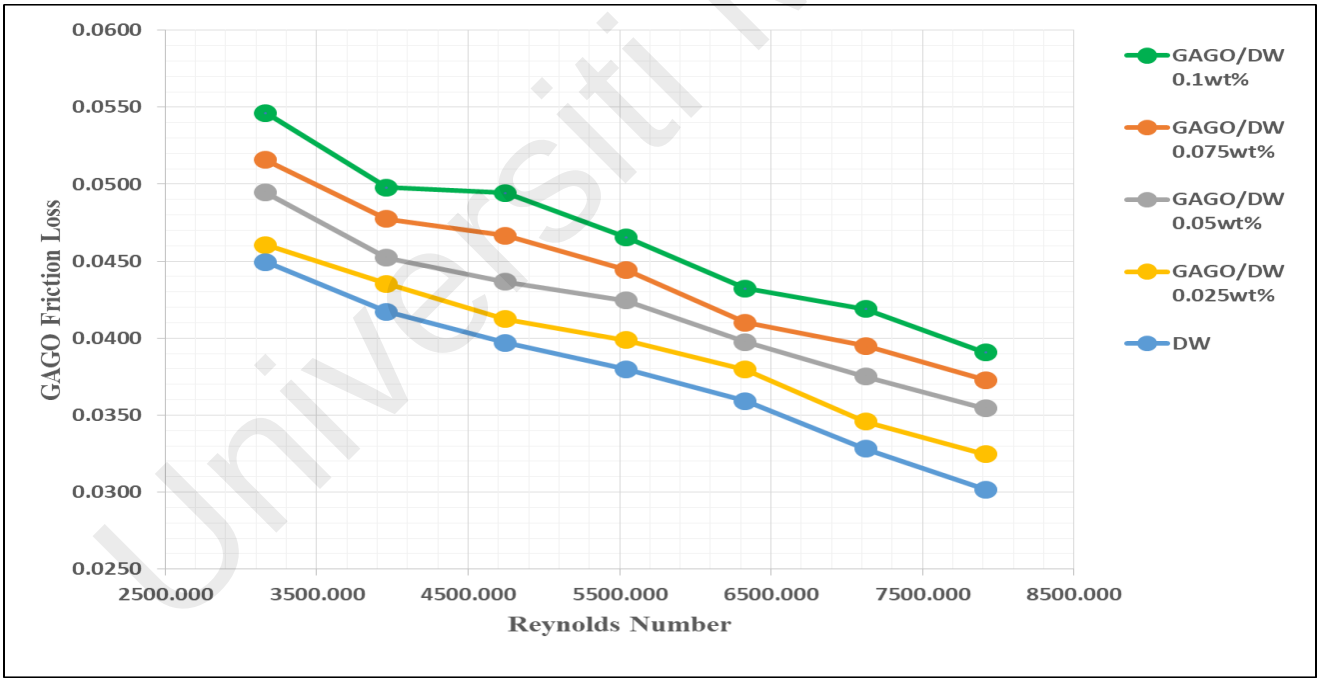

Figure 4.8: Graph of GAGO Friction Loss with DW, 0.025 %, 0.050 % , 0.075% and 0.1% In Annular Test Section

Universiti Malaya

4.2.2.3 Tisi Friction Loss Result in Circular Section

Tisi Friction Loss (Circular)					
Reynolds	TiSi/DW 0.1wt%	TiSi/DW 0.075wt%	TiSi/DW 0.05wt%	TiSi/DW 0.025wt%	DW
13242.2210	0.020400	0.019810	0.018860	0.015880	0.0137
16552.7762	0.017300	0.016560	0.015040	0.013660	0.0123
19863.3314	0.015400	0.013990	0.013160	0.011810	0.0111
23173.8867	0.013100	0.012140	0.011450	0.010450	0.0095
26484.4419	0.012100	0.010770	0.010080	0.009290	0.0082
29794.9971	0.012490	0.010400	0.009570	0.008760	0.0076
33105.5524	0.011600	0.009920	0.009121	0.007670	0.0072

Table 4-7: Table of TiSi Friction Loss with DW, 0.025 %, 0.050 % , 0.075% and 0.1% In Circular Test Section

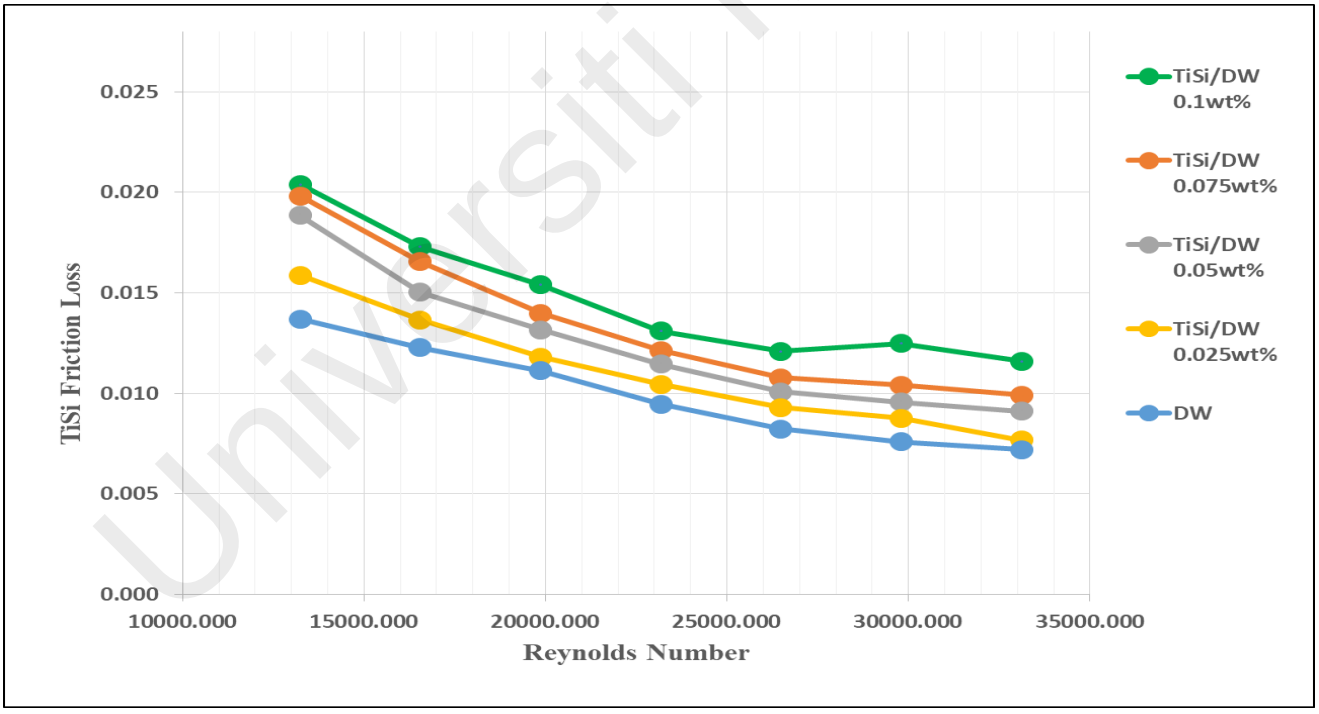

Figure 4.9: Graph of TiSi Friction Loss with DW, 0.025 %, 0.050 % , 0.075% and 0.1% In Circular Test Section

Universiti Malaya

4.2.2.4 Tisi Friction Loss Result in Annular Section

TiSi Friction Loss (Annular)					
Reynolds	TiSi/DW 0.1wt%	TiSi/DW 0.075wt%	TiSi/DW 0.05wt%	TiSi/DW 0.025wt%	DW
3164.0658	0.00297	0.00267	0.00229	0.00185	0.00150
3959.5822	0.00254	0.00201	0.00177	0.00140	0.00104
4747.0987	0.00214	0.00162	0.00133	0.00090	0.00071
5542.6151	0.00174	0.00126	0.00095	0.00073	0.00056
6331.1316	0.00154	0.00108	0.00084	0.00059	0.00034
7125.6480	0.00120	0.00073	0.00058	0.00033	0.00020
7917.1644	0.00104	0.00060	0.00043	0.00028	0.00014

Table 4-8: Table of TiSi Friction Loss with DW, 0.025 %, 0.050 % , 0.075% and 0.1% In Annular Test Section

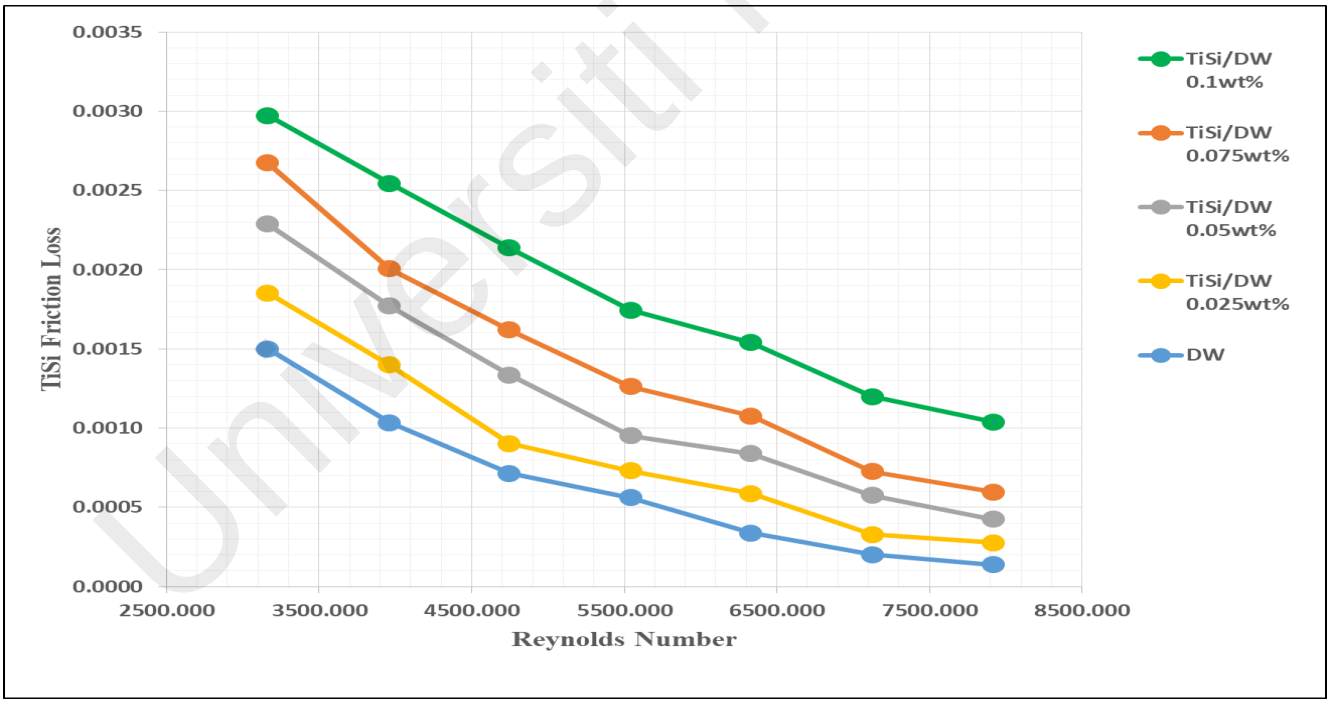

Figure 4.10: Graph of TiSi Friction Loss with DW, 0.025 %, 0.050 % , 0.075% and 0.1% In Annular Test Section

Universiti Malaya

4.2.2.5 Comparison of GAGO Pressure Drop in Circular and Annular Test

GAGO Pressure Drop (Circular and Annular)		
Flowrate	GAGO/DW 0.1wt% (Circular Cross Section)	GAGO/DW 0.1wt% (Annular Cross Section)
4	1898.80	103.11
5	2352.90	146.98
6	2784.70	206.91
7	3521.50	277.54
8	4289.20	310.90
9	5298.30	351.70
10	6228.40	397.20

Table 4-9: Table of Comparison GAGO Pressure Drop with Concentration 0.1%

In Circular and Annular Test Section

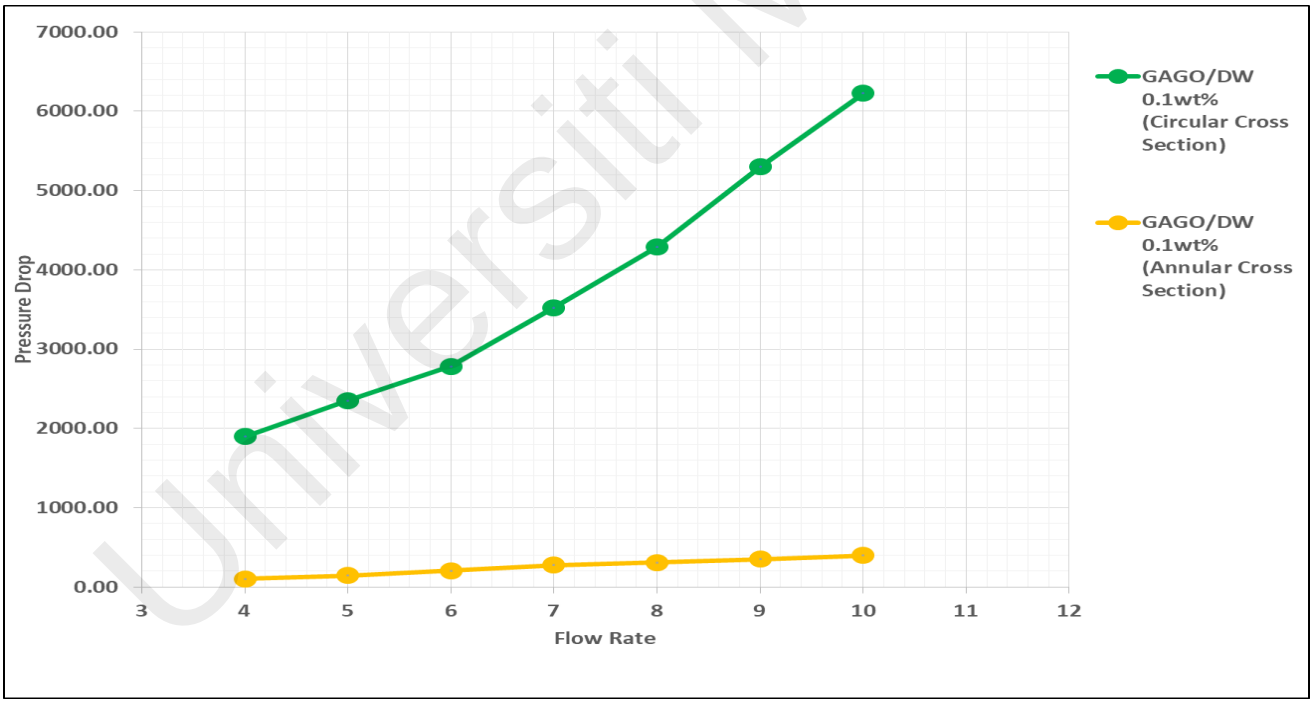

Figure 4.11: Graph of Comparison GAGO Pressure Drop with Concentration 0.1%

In Circular and Annular Test Section

Universiti Malaya

4.2.2.6 Comparison of GAGO Friction loss in Circular and Annular Test

GAGO Friction Loss (Circular and Annular)		
Flowrate	GAGO/DW 0.1wt% (Circular Cross Section)	GAGO/DW 0.1wt% (Annular Cross Section)
4	0.044054989	0.066626275
5	0.034938103	0.060783042
6	0.028715195	0.059420264
7	0.026678872	0.058558345
8	0.024878957	0.050223422
9	0.024282164	0.04489034
10	0.023121305	0.04106528

Table 4-10: Table of Comparison GAGO Friction Loss with Concentration 0.1%

In Circular and Annular Test Section

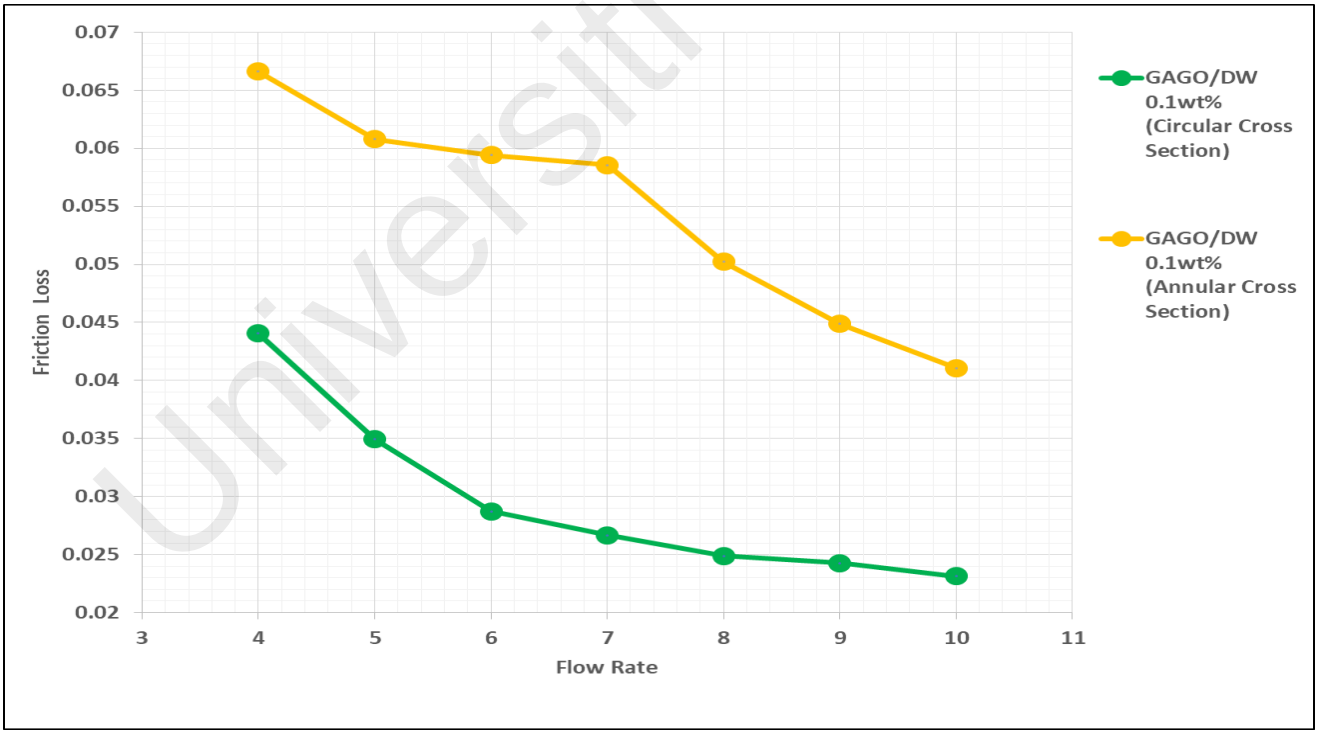

Figure 4.12: Graph of Comparison GAGO Friction Loss with Concentration 0.1%

In Circular and Annular Test Section

Universiti Malaya

4.2.2.7 Comparison of Tisi Pressure Drop in Circular and Annular Test

TiSi Pressure Drop (Circular and Annular)		
Flowrate	TiSi /DW 0.1wt% (Circular Cross Section)	TiSi /DW 0.1wt% (Annular Cross Section)
4	1995.90	96.00
5	2427.20	108.32
6	3089.30	121.60
7	3811.80	136.30
8	4604.60	149.60
9	5625.80	161.50
10	6630.20	171.40

Table 4-11: Table of Comparison TiSi Pressure Drop with Concentration 0.1%

In Circular and Annular Test Section

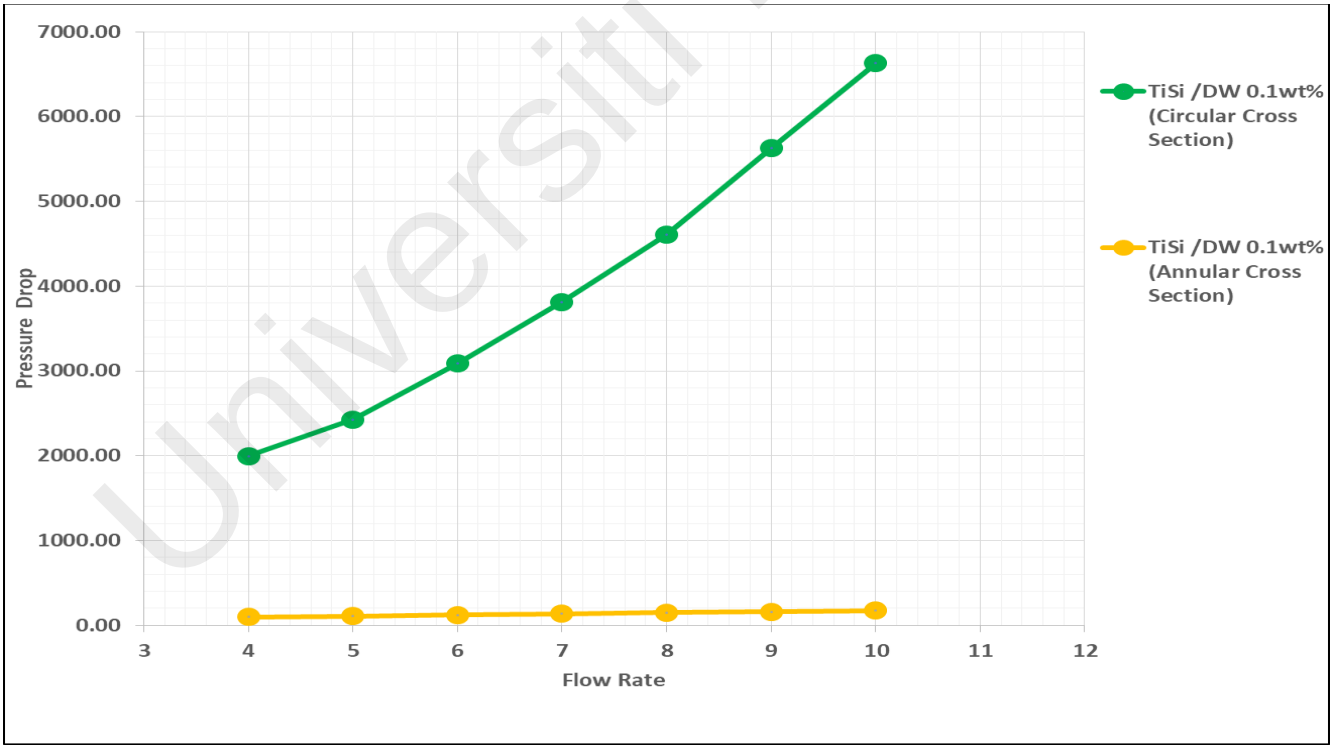

Figure 4.13: Graph of Comparison TiSi Pressure Drop with Concentration 0.1%

In Circular and Annular Test Section

Universiti Malaya

4.2.2.8 Comparison of Tisi Friction loss in Circular and Annular Test

TiSi Friction Loss (Circular and Annular)		
Flow Rate	TiSi /DW 0.1wt% (Circular Cross Section)	TiSi/DW 0.1wt% (Annular Cross Section)
4	0.0204	0.002971796
5	0.0173	0.002544852
6	0.0154	0.00213719
7	0.0131	0.001744973
8	0.0121	0.001539197
9	0.01249	0.001197979
10	0.0116	0.001039395

Table 4-12: Table of Comparison TiSi Friction Loss with Concentration 0.1%

In Circular and Annular Test Section

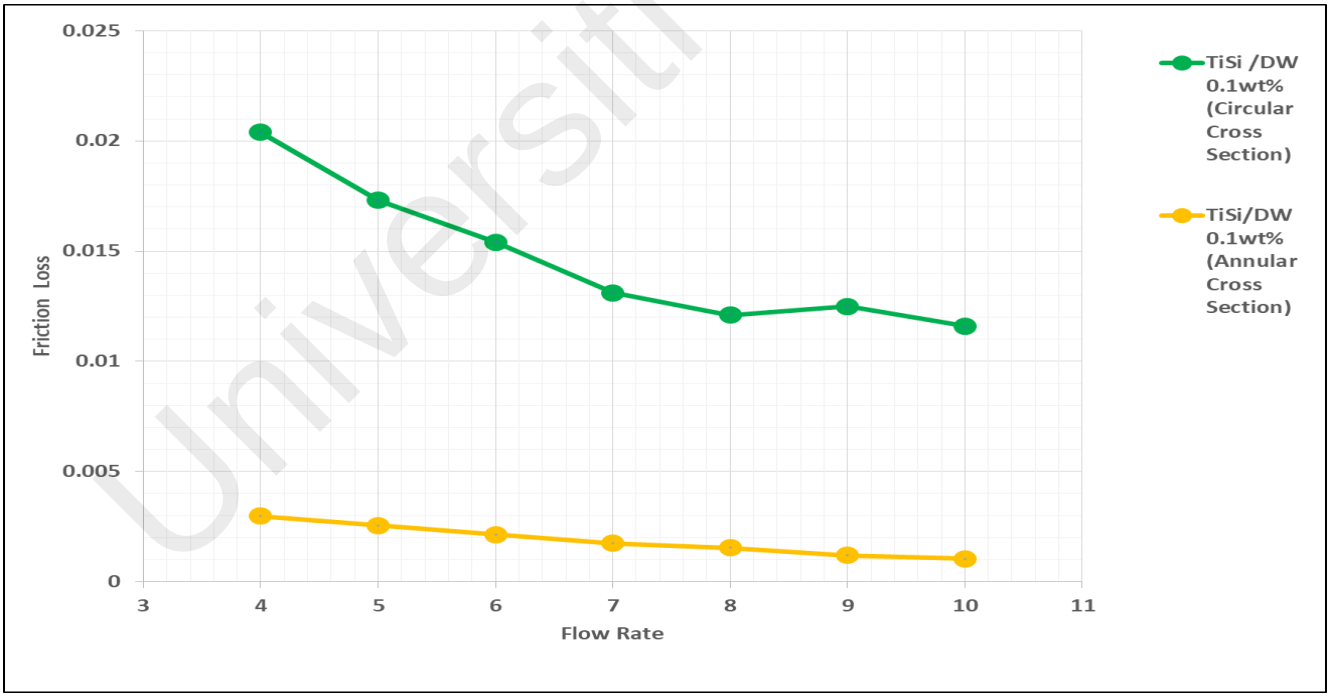

Figure 4.14: Graph of Comparison TiSi Friction loss with Concentration 0.1%

In Circular and Annular Test Section

Universiti Malaya

4.2.3 Pumping Power of GAGO /DW

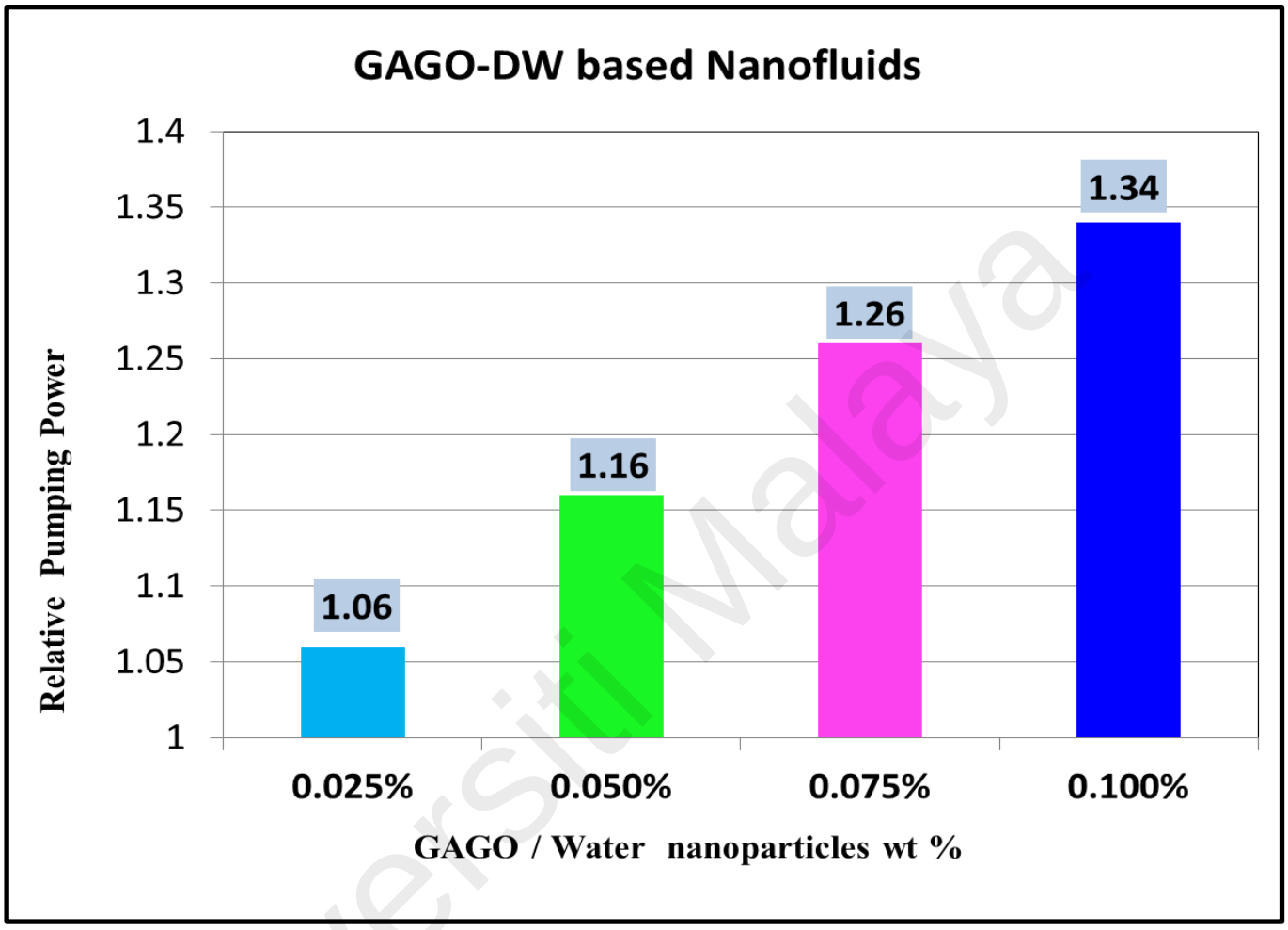

Figure 4.15: Graph of GAGO /DW Pumping Power with Concentration 0.025% ,0.500% , 0.075% and 0.100%

Based on Figure 4.15 The relative pumping power Keep increasing when the concentration of GAGO Nanofluid increase.

Universiti Malaya

4.2.4 Pumping Power of TiSi /DW

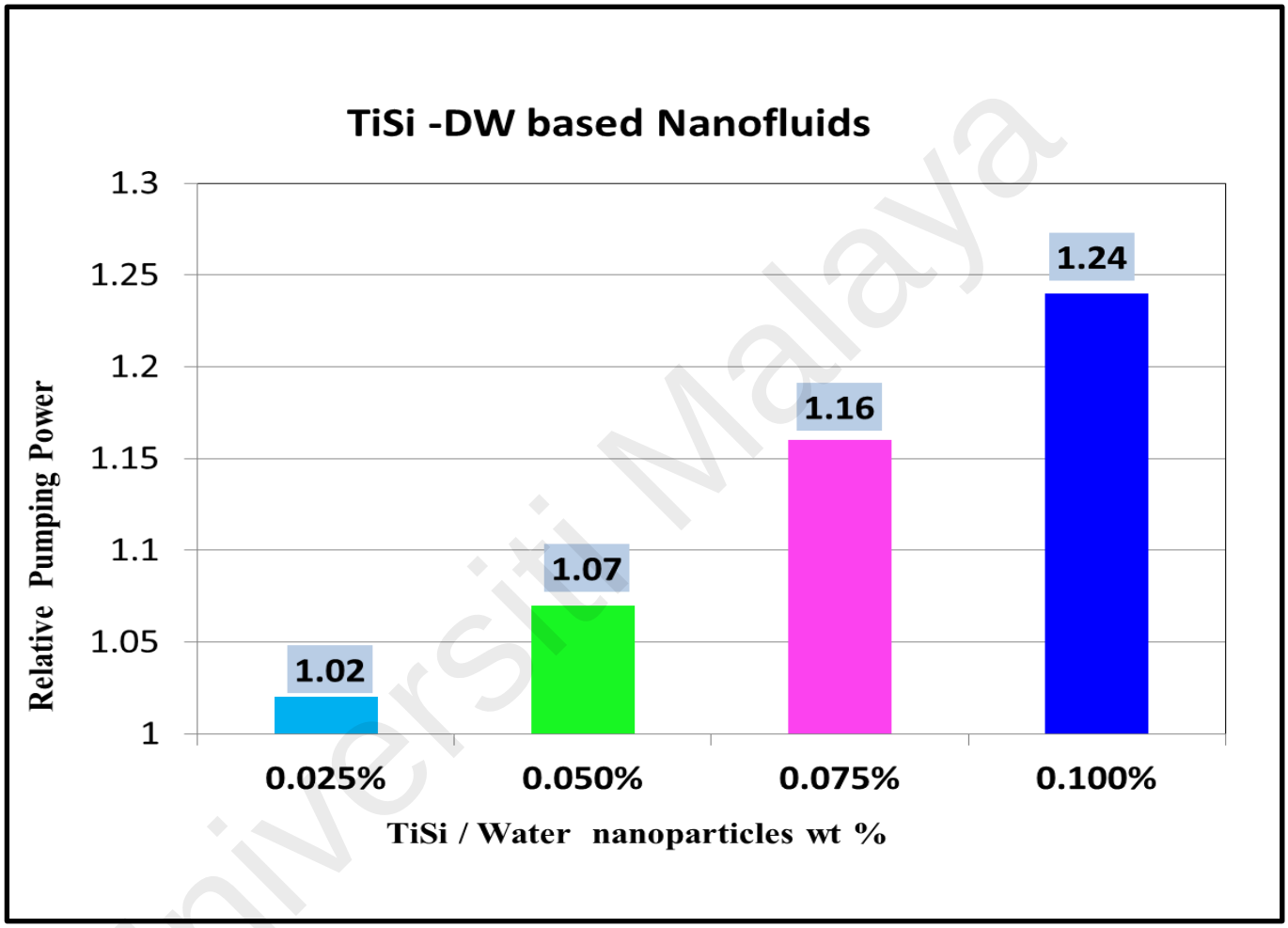

Figure 4.16: Graph of TiSi /DW Pumping Power with Concentration 0.025%,0.500% ,0.075% and 0.100%

Based on Figure 4.16 The relative pumping power Keep increasing when the concentration of TiSi Nanofluid increase.

Universiti Malaya

4.3 Heat Transfer Properties

4.3.1Average Heat Transfer of the GAGO/DW based nanofluids in circular test section

GAGO Heat Transfer Coefficient (Circular)					
Reynolds	GAGO/DW 0.1wt%	GAGO/DW 0.075wt%	GAGO/DW 0.05wt%	GAGO/DW 0.025wt%	DW
13202.494	753.5198	722.1685	629.3126	537.5399	536.6454
16503.118	747.9469	726.7372	654.5857	593.5237	583.8218
19803.741	774.7400	758.1136	717.6678	656.5080	635.9310
23104.365	784.2509	772.1092	734.3875	675.7456	662.8856
26404.989	866.1232	836.7768	792.9933	755.2099	738.5670
29705.612	1129.3115	1060.5924	1000.4132	940.1672	837.2404
33006.236	1315.5273	1254.0287	1205.4105	1099.3256	1046.8099

Table 4-13: Table of GAGO Heat Transfer Coefficient with DW, 0.025 %, 0.050 % , 0.075% and 0.1% In Circular Test Section

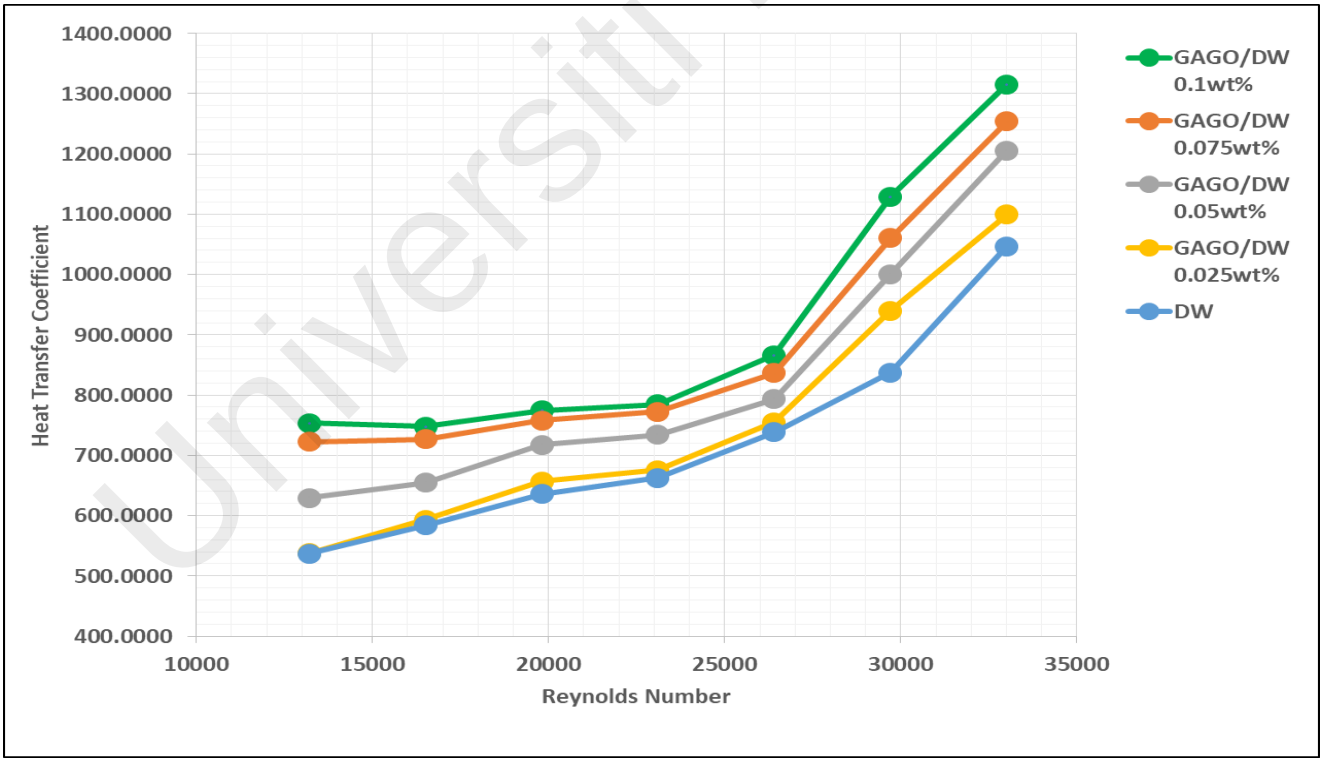

Figure 4-17: Graph of GAGO Heat Transfer Coefficient with DW, 0.025 %, 0.050 % , 0.075% and 0.1% Circular Test Section

Universiti Malaya

4.3.2 Average Heat Transfer of the TiO2+SiO2/DW based nanofluids in circular test section

TiSi Heat Transfer Coefficient (Circular)					
Reynolds	TiSi/DW 0.1wt%	TiSi /DW 0.075wt%	TiSi /DW 0.05wt%	TiSi /DW 0.025wt%	DW
13242.221	604.4733	572.2554	557.4662	527.8499	504.9111
16552.776	616.5617	582.1893	555.4205	533.8944	519.7114
19863.331	638.6867	596.5162	588.2086	566.1288	535.5383
23173.887	650.5023	620.4942	608.0809	584.3917	556.4315
26484.442	670.5714	651.7373	612.3853	607.8596	557.5965
29794.997	679.2350	669.1234	645.9309	630.9020	572.4924
33105.552	724.2584	692.6950	667.7272	656.5198	588.9931

Table 4-14: Table of TiSi Heat Transfer Coefficient with DW, 0.025 %, 0.050 % , 0.075% and 0.1% In Circular Test Section

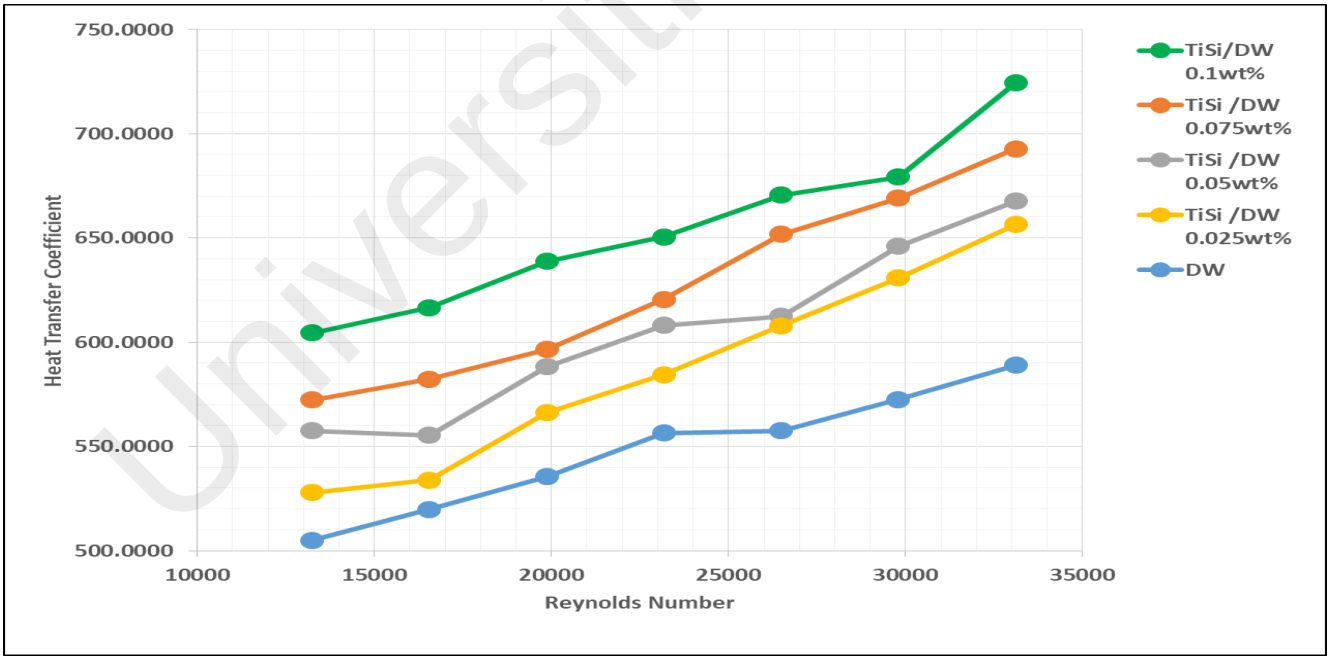

Figure 4-18: Graph of TiSi Heat Transfer Coefficient with DW, 0.025 %, 0.050 % , 0.075% and 0.1% In Circular Test Section

Universiti Malaya

4.3.3 Average Nusslet Numbers of the GAGO/DW based nanofluids in Cirular test section

GAGO Average Nusselt Number (Circular)					
Reynolds	GAGO/DW 0.1wt%	GAGO/DW 0.075wt%	GAGO/DW 0.05wt%	GAGO/DW 0.025wt%	DW
13202.494	12.2524	11.7426	10.2327	8.7405	8.7259
16503.118	12.1617	11.8169	10.6437	9.6508	9.4930
19803.741	12.5974	12.3270	11.6694	10.6749	10.3403
23104.365	12.7520	12.5546	11.9413	10.9877	10.7786
26404.989	13.5955	13.2809	12.8942	12.2798	12.0092
29705.612	18.3628	17.2454	16.2669	15.9377	13.6137
33006.236	21.3907	20.3907	19.6002	19.5012	17.0213

Table 4-15: Table of GAGO Average Nusselt Number with DW, 0.025 %, 0.050 % , 0.075% and 0.1% In Circular Test Section

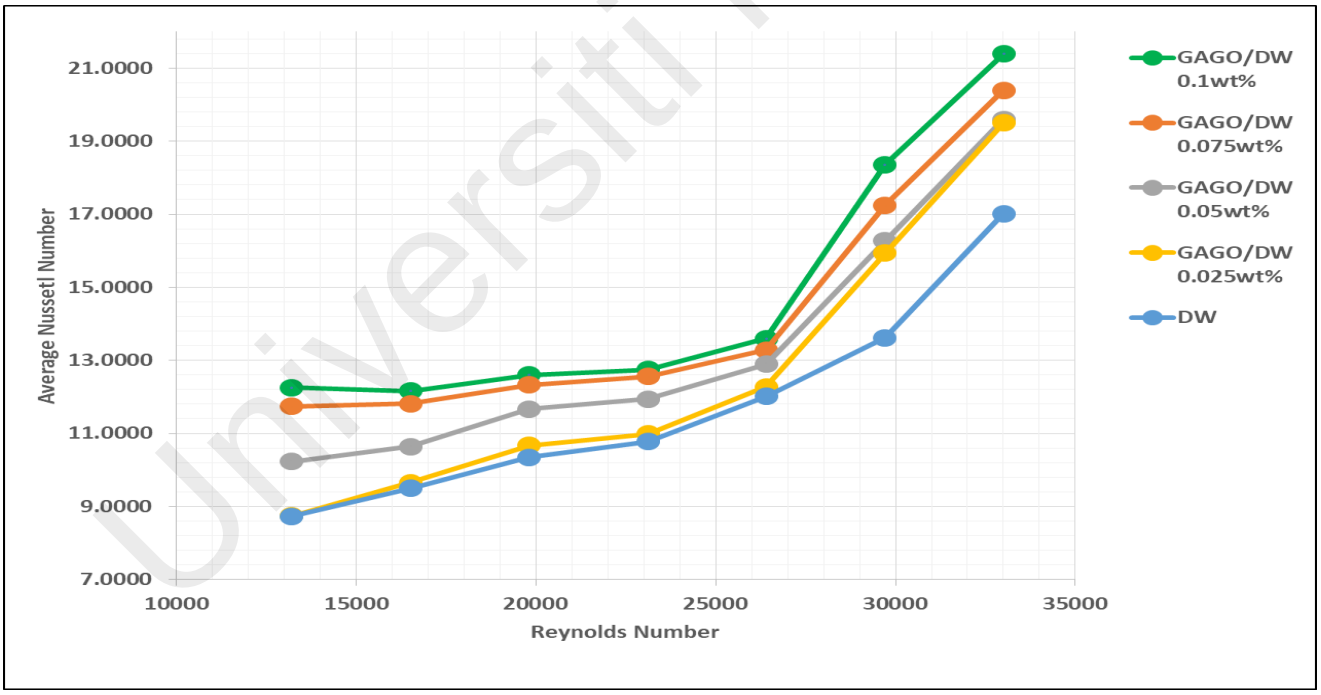

Figure 4-19: Graph of GAGO Average Nusselt Number with DW, 0.025 %, 0.050 % , 0.075% and 0.1% In Circular Test Section

Universiti Malaya

4.3.4 Average Nusslet Numbers of the TiO2+SiO2/DW based nanofluids in Cirular test section

Average Nusselt Number					
Reynolds	TiSi/DW 0.1wt%	TiSi /DW 0.075wt%	TiSi /DW 0.05wt%	TiSi /DW 0.025wt%	DW
13242.221	9.0333	8.4641	7.9272	7.6808	7.2099
16552.776	8.9422	8.5405	8.0450	7.8979	7.6376
19863.331	9.0709	8.7919	8.5716	8.3807	7.9819
23173.887	9.3958	9.0828	8.8353	8.5249	8.2460
26484.442	9.8091	9.4112	9.2107	8.9779	8.4406
29794.997	10.0838	9.5544	9.2919	8.9862	8.7324
33105.552	10.9629	10.1279	9.8254	9.4670	9.3007

Table 4-16: Table of TiSi Average Nusselt Number with DW, 0.025 %, 0.050 % , 0.075% and 0.1% In Circular Test Section

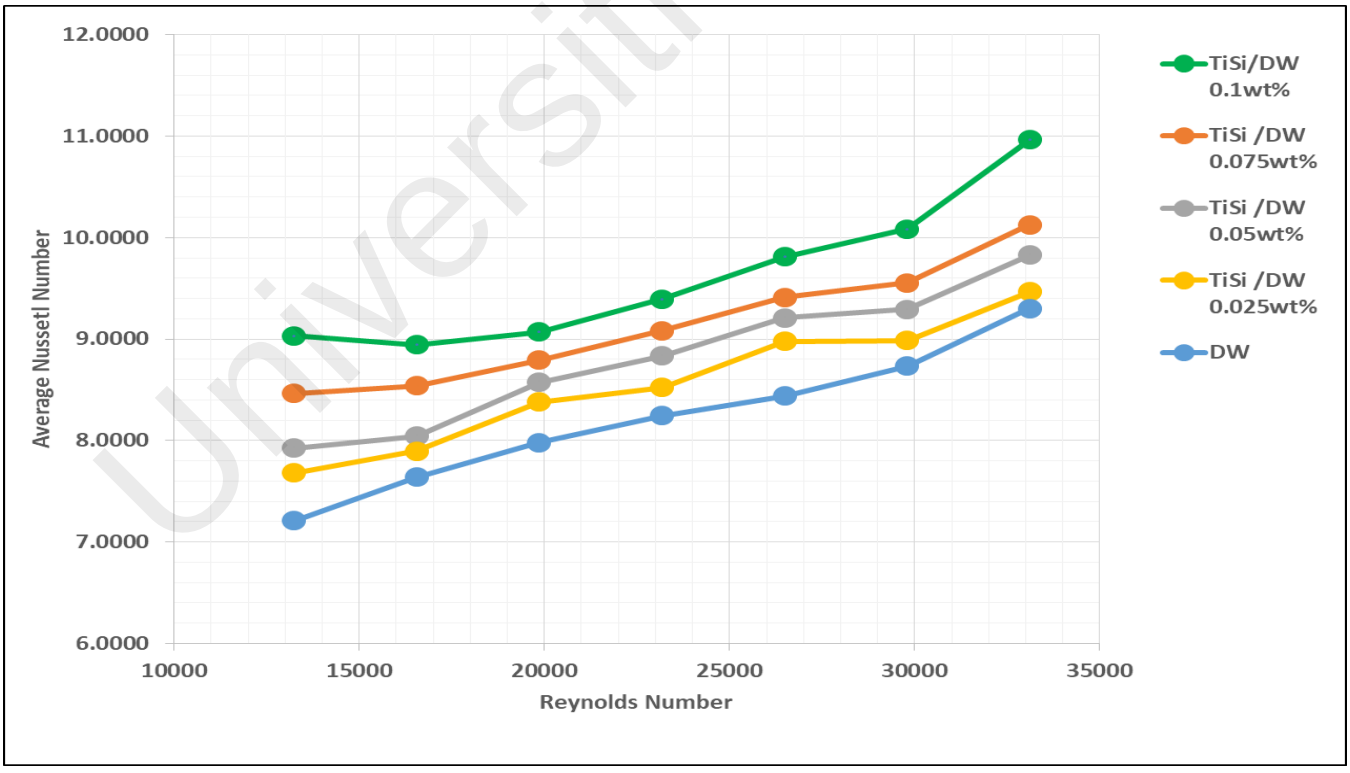

Universiti Malaya

Figure 4-20: Graph of TiSi Average Nusselt Number with DW, 0.025 %, 0.050 % , 0.075% and 0.1% In Circular Test Section

4.3.5 Average Heat Transfer of the GAGO/DW based nanofluids in annular test section

GAGO Heat Transfer Coefficient (Annular)					
Reynolds	GAGO/DW 0.1wt%	GAGO/DW 0.075wt%	GAGO/DW 0.05wt%	GAGO/DW 0.025wt%	DW
3166.0658	423.4866	407.5255	393.4432	370.1475	358.5866
3957.5822	522.7934	492.7414	472.5744	447.8877	431.0327
4749.0987	552.5885	499.1956	488.0326	478.4144	459.0522
5540.6151	565.4364	525.2726	518.2464	507.1091	480.9195
6332.1316	600.0155	557.2175	542.5729	526.3583	510.8558
7123.6480	645.4921	604.3862	592.7307	571.2162	552.9491
7915.1644	695.7854	646.2524	619.1425	605.2971	584.6249

Table 4-17: Table of GAGO Heat Transfer Coefficient with DW, 0.025 %, 0.050 % , 0.075% and 0.1% In Annular Test Section

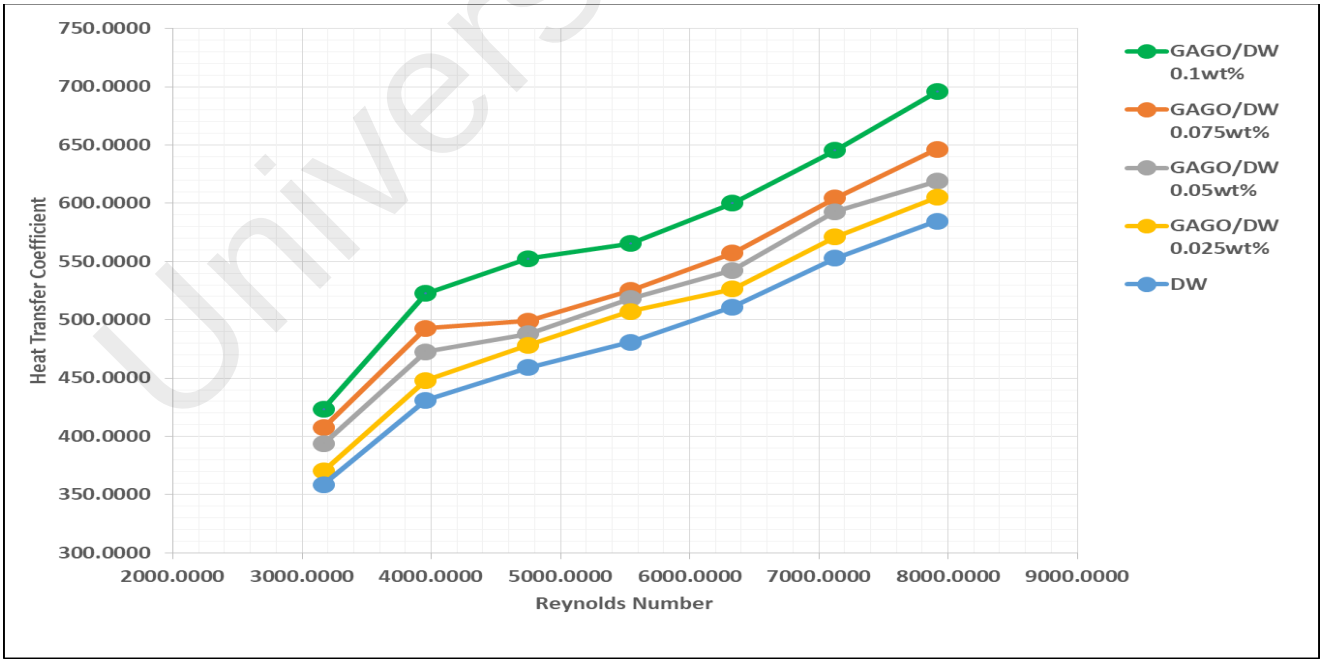

Universiti Malaya

Figure 4-21: Graph of GAGO Heat Transfer Coefficient with DW, 0.025 %, 0.050 % , 0.075% and 0.1% In Annular Test Section

4.3.6 Average Heat Transfer of the TiO2+SiO2/DW based nanofluids in annular test section

TiSi Heat Transfer Coefficient (Annular)					
Reynolds	TiSi/DW 0.1wt%	TiSi /DW 0.075wt%	TiSi /DW 0.05wt%	TiSi/DW 0.025wt%	DW
15446.9183	732.4316	672.1070	615.9631	559.0098	489.3592
19308.6479	737.1869	694.9120	646.9273	561.9480	528.4390
23170.3775	752.1495	688.0243	658.9168	572.6823	560.4130
27032.1071	797.2019	731.3649	661.5153	592.4648	578.3477
30893.8366	816.3693	744.3493	686.5388	584.0702	574.7610
34755.5662	843.1836	768.6955	698.6420	609.0117	588.3710
38617.2958	889.5552	775.9580	734.5415	622.9447	612.4282

Table 4-18: Table of TiSi Heat Transfer Coefficient with DW, 0.025 %, 0.050 % , 0.075% and 0.1% In Annular Test Section

Universiti Malaya

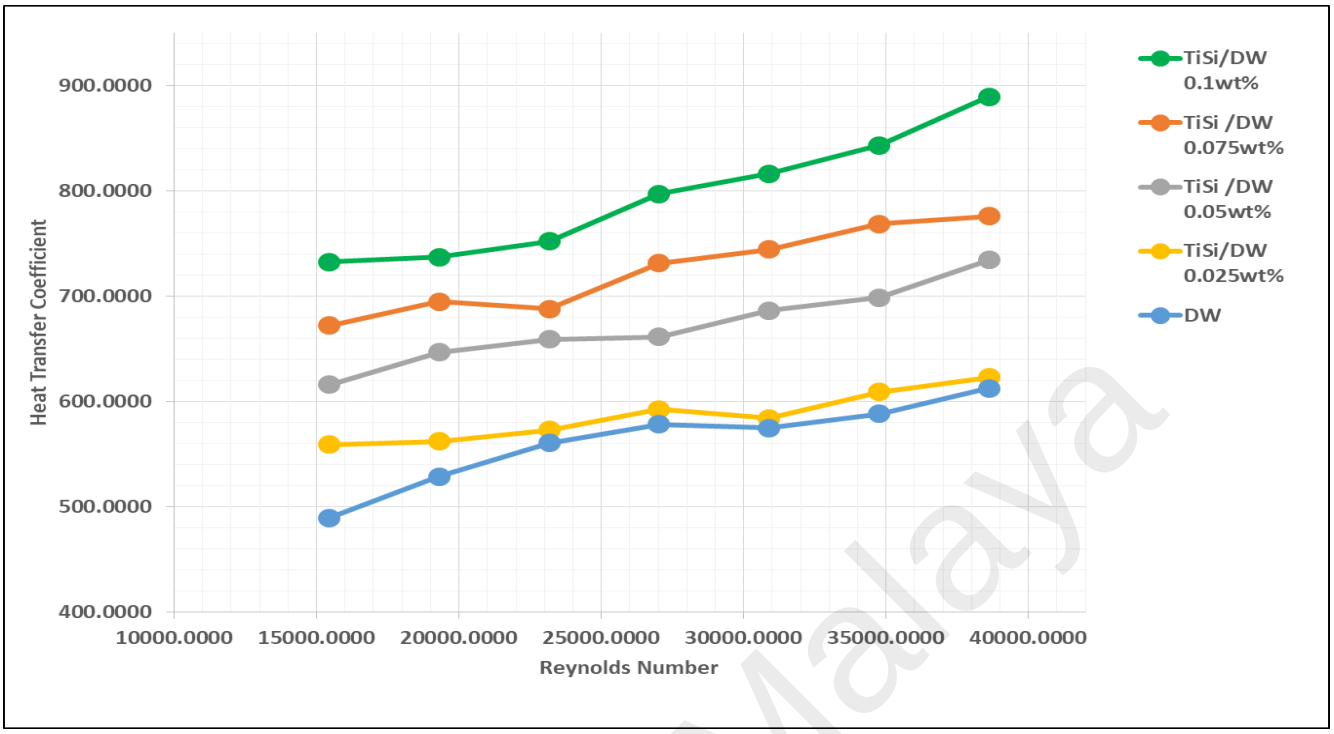

Figure 4-22: Graph of TiSi Heat Transfer Coefficient with DW, 0.025 %, 0.050 % , 0.075% and 0.1% In Annular Test Section

4.3.7 Average Nusslet Numbers of the GAGO/DW based nanofluids in annular test section

GAGO Average Nusselt Number (Annular)					
Reynolds	GAGO/DW 0.1wt%	GAGO/DW 0.075wt%	GAGO/DW 0.05wt%	GAGO/DW 0.025wt%	DW
3166.0658	8.05657	7.75292	7.48502	7.04183	6.82189
3957.5822	9.94583	9.33411	8.99044	8.51079	8.20013
4749.0987	10.51266	9.49689	9.28452	9.10154	8.73319
5540.6151	10.75708	9.99299	9.85932	9.64744	9.09481
6332.1316	11.41493	10.52072	10.26012	9.97850	9.71872
7123.6480	12.28009	11.49808	11.40951	10.84704	10.51952
7915.1644	13.23689	12.29456	11.77881	11.51541	11.12213

Table 4-19: Table of GAGO Average Nusselt Number with DW, 0.025 %, 0.050 % , 0.075% and 0.1% In Annular Test Section

Universiti Malaya

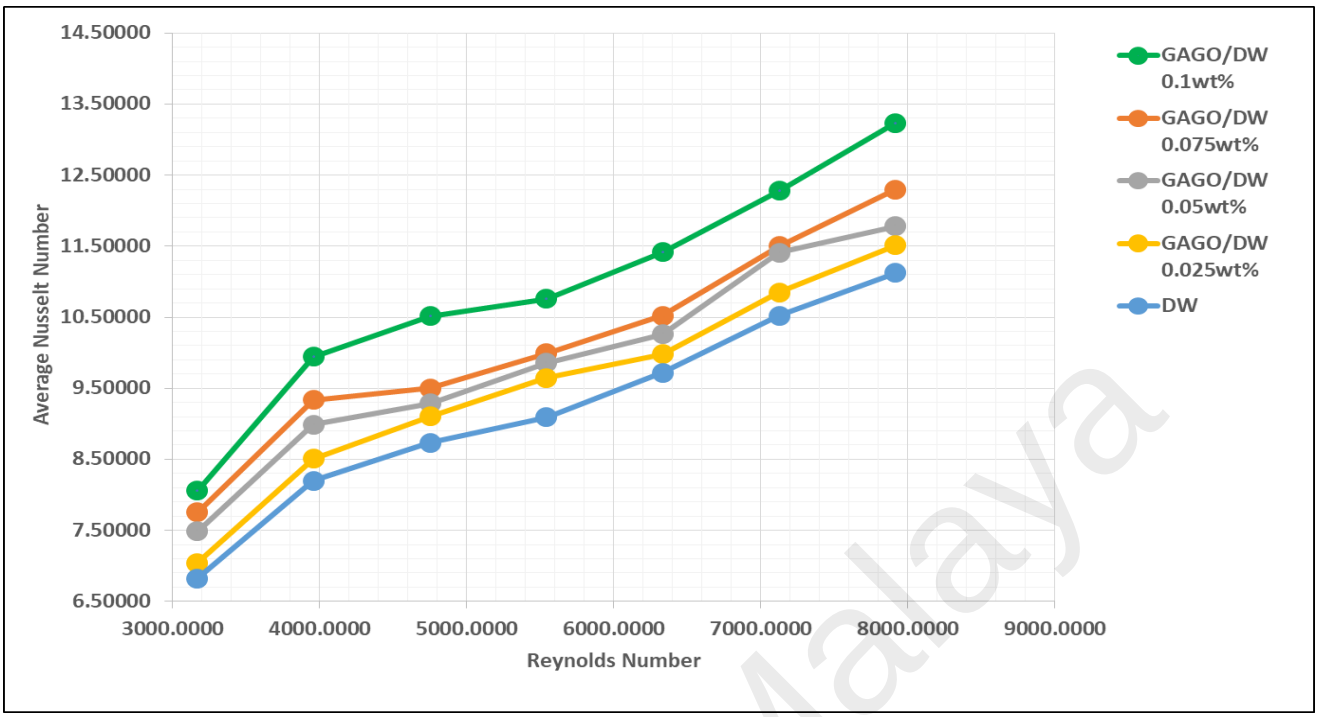

Figure 4-23: Graph of GAGO Average Nusselt Number with DW, 0.025 %, 0.050 % , 0.075% and 0.1% In Annular Test Section

4.3.8 Average Nusslet Numbers of the TiO2+SiO2/DW based nanofluids in annular test section

TiSi Average Nusselt Number (Annular)					
Reynolds	TiSi/DW 0.1wt%	TiSi /DW 0.075wt%	TiSi /DW 0.05wt%	TiSi/DW 0.025wt%	DW
15446.9183	11.99082	10.59348	9.98098	8.52584	7.40732
19308.6479	12.32782	11.16879	10.63605	9.27035	8.15079
23170.3775	12.38506	11.11638	10.49518	9.36357	8.75908
27032.1071	12.84424	11.63206	10.61745	9.92325	9.42369
30893.8366	13.04182	12.46573	11.37725	10.67040	10.17350
34755.5662	13.49348	12.87837	12.58102	11.97337	10.88901
38617.2958	14.07070	13.34246	12.90396	11.97541	11.65107

Table 4-20: Table of TiSi Average Nusselt Number with DW, 0.025 %, 0.050 % , 0.075% and 0.1% In Annular Test Section

Universiti Malaya

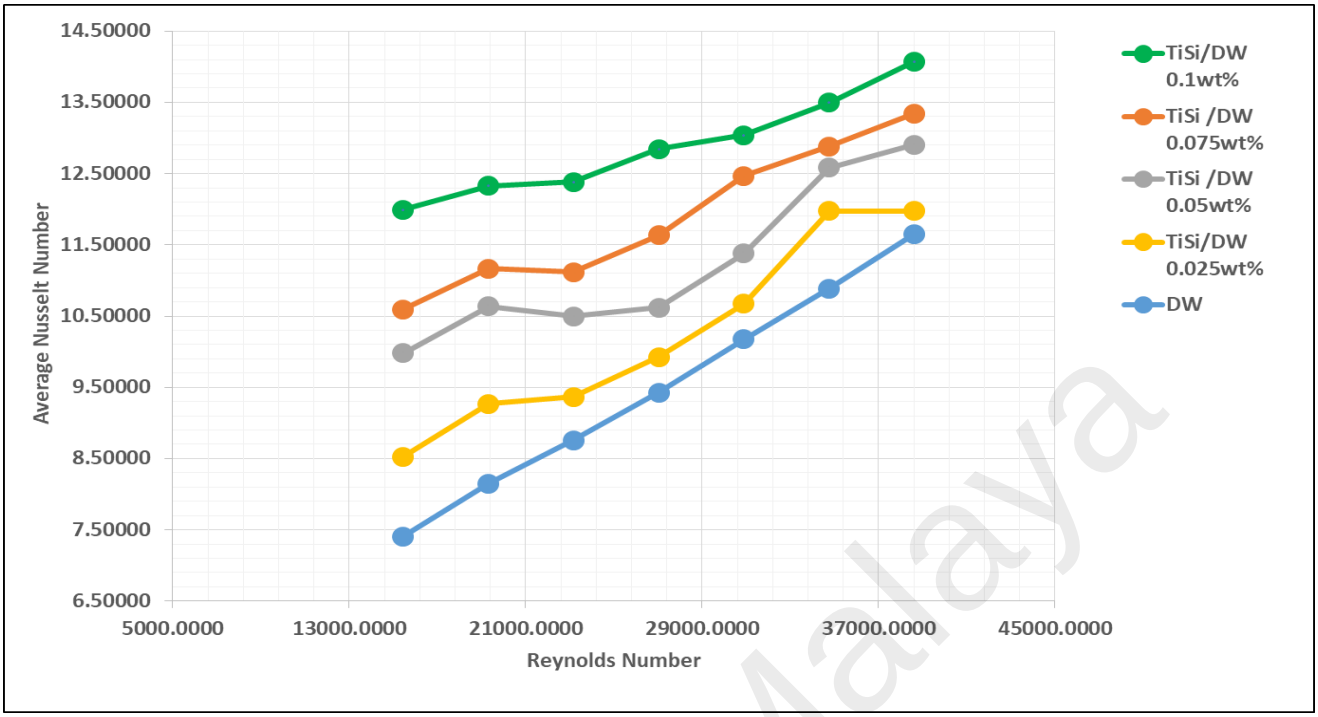

Figure 4-24: Graph of TiSi Average Nusselt Number with DW, 0.025 %, 0.050 % , 0.075% and 0.1% In Annular Test Section

4.3.9 Comparison of heat transfer improvement of both circular and annular test section for GAGO/DW based nanofluids.

Heat Transfer Coefficient		
Flowrate	GAGO/DW 0.1wt% (Circular Cross Section)	GAGO/DW 0.1wt% (Annular Cross Section)
4	753.52	423.49
5	747.95	522.79
6	774.74	552.59
7	784.25	565.44
8	836.12	600.02
9	1129.31	645.49
10	1315.53	695.79

Table 4-21: Table of Comparison GAGO heat transfer Coefficient with Concentration 0.1%

Universiti Malaya

In Circular and Annular Test Section

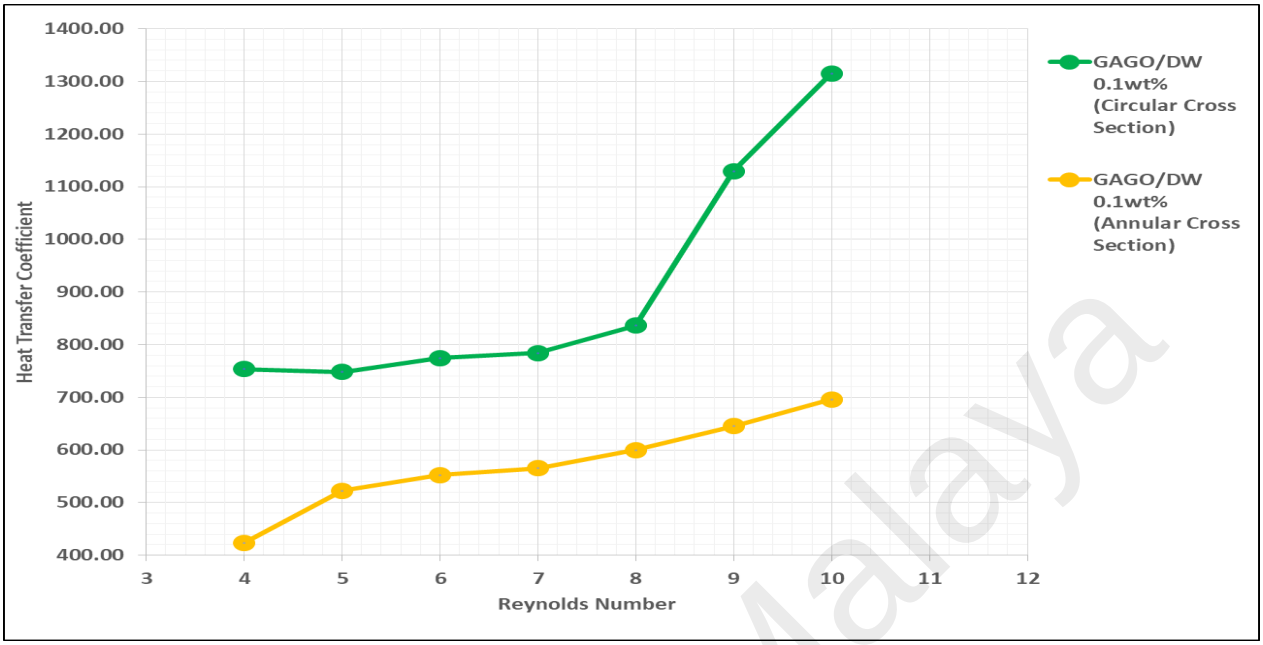

Figure 4-25: Graph of Comparison GAGO heat transfer Coefficient with Concentration 0.1%

In Circular and Annular Test Section

4.3.10 Comparison of heat transfer improvement of both circular and annular test section for TiO2+SiO2/DW based nanofluids.

Heat Transfer Coefficient		
Flowrate	TiSi/DW 0.1wt% (Circular Cross Section)	TiSi/DW 0.1wt% (Annular Cross Section)
4	604.47	732.43
5	616.56	737.19
6	638.69	752.15
7	650.50	797.20
8	670.57	816.37
9	679.23	843.18
10	724.26	889.56

Table 4-22: Table of Comparison TiSi heat transfer Coefficient with Concentration 0.1%

In Circular and Annular Test Section

Universiti Malaya

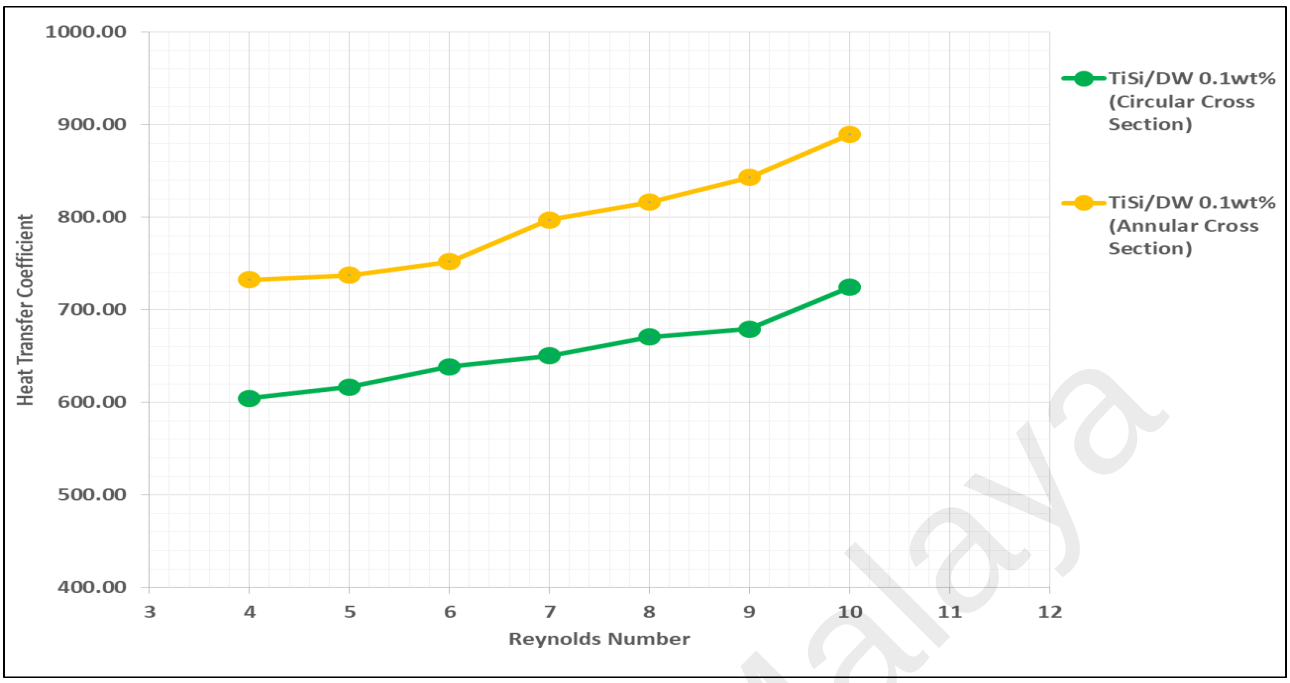

Figure 4.26: Table of Comparison TiSi heat transfer Coefficient with Concentration 0.1%

In Circular and Annular Test Section

Universiti Malaya

CHAPTER 5: CONCLUSION

In this investigation all the objectives were achieved, and they are in depth described in the Results and discussion sections of this thesis. General conclusions of the research output are presented here.

I. From the investigation it has established that higher heat transfer coefficient could be obtained in a circular tube in comparison to the annular flow passage.

II. It was observed that the concentration of Nanofluids has a dominating effect on the heat transfer characteristics of the working fluid. The higher the concentration , the greater the capacity for the heat transfer. In the present investigation the highest concentration of GNP 0.1 percent has shown the highest. Nusslet Number and heat Transfer coefficients compared with the data of lower concentration nanofluids of GNP.

III. Thermal conductivities evaluated were verified by the analytical equations and found satisfactory results and similarities.

5.1 Recommendation on Future Work

The current effort is solely aimed at improving the working fluid. More research is needed to determine the best base fluid, such as distilled water or any oil-based fluid, to enhance total heat transfer and for specific applications. Aside from that, the material used to make the heat exchanger must be considered. For significantly increased cooling, materials with higher heat conductivity will be employed. Composites of the nanoparticles of GNPs with metals or metal oxides could be investigated for multipurpose applications.

Universiti Malaya

CHAPTER 6: REFERENCE

1. Khanafer, K.; Vafai, K. A review on the applications of nanofluids in solar energy field. *Renew. Energy* 2018, *123*, 398–406.

2. Elsheikh, A.; Sharshir, S.; Mostafa, M.E.; Essa, F.; Ali, M.K.A. Applications of nanofluids in solar energy: A review of recent advances. *Renew. Sustain. Energy Rev.* 2018, *82*, 3483–3502.

3. Akram, N.; Sadri, R.; Kazi, S.N.; Ahmed, S.M.; Zubir, M.N.M.; Ridha, M.; Soudagar, M.; Ahmed, W.; Arzpeyma, M.; Tong, G.B. An experimental investigation on the performance of a flat-plate solar collector using eco-friendly treated graphene nanoplatelets–water nanofluids. *J. Therm. Anal. Calorim.* 2019, *138*, 609–621.

4. Sharafeldin, M.A.; Gróf, G. Efficiency of evacuated tube solar collector using WO3/Water nanofluid. *Renew. Energy* 2019, *134*, 453–460.

5. Zhu, H.; Zhang, C.; Tang, Y.; Wang, J.; Ren, B.; Yin, Y. Preparation and thermal conductivity of suspensions of graphite nanoparticles. *Carbon* 2007, *45*, 226–228.

Universiti Malaya

6. Sridhar, V., Jeon, J.-H., & Oh, I.-K. (2010). Synthesis of graphene nano-sheets using eco-friendly chemicals and microwave radiation. Carbon, 48(10), 2953-2957. doi:https://doi.org/10.1016/j.carbon.2010.04.034

7. Sadri, R., Hosseini, M., Kazi, S. N., Bagheri, S., Zubir, N., Ahmadi, G., . . . Zaharinie, T. (2017). A novel, eco-friendly technique for covalent functionalization of graphene nanoplatelets and the potential of their nanofluids for heat transfer applications (Vol. 675).

8. Wong, K. V., & De Leon, O. (2010). Applications of Nanofluids: Current and Future. Advances in Mechanical Engineering, 2, 519659. doi:10.1155/2010/519659

9. Zhu, H., Zhang, C., Tang, Y., Wang, J., Ren, B., & Yin, Y. (2007). Preparation and thermal conductivity of suspensions of graphite nanoparticles. Carbon, 45, 226-228. doi:10.1016/j.carbon.2006.07.005

10. Yu, W., Xie, H., & Bao, D. (2009). Enhanced thermal conductivities of nanofluids containing graphene oxide nanosheets. Nanotechnology, 21(5), 055705. doi:10.1088/0957-4484/21/5/055705

11. Huminic, G., & Huminic, A. (2012). Application of nanofluids in heat exchangers: A review. *Renewable and Sustainable Energy Reviews, 16*(8), 5625-5638. doi:https://doi.org/10.1016/j.rser.2012.05.023

Universiti Malaya

12. Xuan, Y., & Roetzel, W. (2000). Conceptions for heat transfer correlation of nanofluids. International Journal of Heat and Mass Transfer, 43(19), 3701-3707. doi:https://doi.org/10.1016/S0017-9310(99)00369-5

13. Wang, X.-Q., & Mujumdar, A. S. (2008). A review on nanofluids - part II: experiments and applications. Brazilian Journal of Chemical Engineering, 25, 631-648.
Second edition of the Encyclopædia Britannica (1777–84), title page of volume10.Encyclopædia Britannica, Incdoi:https:shell-and-tube-heat-exchanger.html.

14. Guo Preparation, characterization and catalytic performance of core–shell Cu-Ce-La-SSZ-13[D] , Nanjing University of Science and Technology, 2018

15. Study on the mechanism of synthetic (Ce,La)CO3F sulfuric acid acidification and NH3-SCR loaded with Mn and Fe(Na Li, Zedong Chen, Xinrui Bai, Limin Hou, Kunling Jiao and Wenfei Wu)

16. Alawi, Omer A., et al. "Graphene Nanoplatelets Suspended in Different Basefluids Based Solar Collector: An Experimental and Analytical Study." *Processes* 9.2 (2021): 302.

17. Alawi, O.A., Kamar, H.M., Mallah, A.R., Mohammed, H.A., Sabrudin, M.A.S., Hussein, O.A., Kazi, S.N. and Najafi, G., 2021. Graphene Nanoplatelets Suspended in Different Basefluids Based Solar Collector: An Experimental and Analytical Study. *Processes*, *9*(2), p.302.

Universiti Malaya

18. Alawi, Omer A., Haslinda Mohamed Kamar, Abdul Rahman Mallah, Hussein A. Mohammed, Mohd Aizad Sazrul Sabrudin, Omar A. Hussein, Salim Newaz Kazi, and Gholamhassan Najafi. "Graphene Nanoplatelets Suspended in Different Basefluids Based Solar Collector: An Experimental and Analytical Study." *Processes* 9, no. 2 (2021): 302. Safaei, Mohammad Reza, et al. "A survey on experimental and numerical studies of convection heat transfer of nanofluids inside closed conduits." *Advances in Mechanical Engineering* 8.10 (2016): 1687814016673569.

Universiti Malaya